

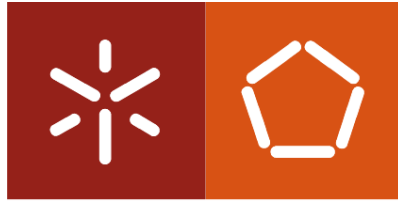
Universidade do Minho

Escola de Engenharia

Ângela Filipa Esteves Machado Fontela

**Protein effect on the corrosion
behaviour of titanium modified by two
surface treatments**

October 2011



Universidade do Minho

Escola de Engenharia

Ângela Filipa Esteves Machado Fontela

**Protein effect on the corrosion
behaviour of titanium modified by two
surface treatments**

Tese de Mestrado em Engenharia Biomédica
Ramo de Biomateriais, Reabilitação e Biomecânica

Trabalho realizado sob a orientação de
**Professor Doutor Luís Augusto Sousa Marques
da Rocha**
Professor Doutor Jean-Pierre Celis

October 2011

Acknowledgements

I would like to offer my sincerest gratitude to my supervisor Prof. Dr. Ir. Luís Rocha from Universidade do Minho, Guimarães, Portugal; and to Prof. Dr. Ir. Jean-Pierre Celis from Katholic Universiteit Leuven, Belgium for his guidance and wise advice throughout all the process of this work.

The Group CT2M which provided the materials and equipment needed to produce and complete this project.

To Alexandra Alves, Helena Cruz, Maria João Runa, Fernando Oliveira, Ana Lúcia Roselino and Jeferson Moreto for all the patience and help, for teaching me how to get around in the lab, for the friendship and good moments offered.

To Abdenacer Berradja, Natali Tintaru, Houcine Dhieb, Wassim Zeineddine, Mark Pieters, Berkay Kavas, Emmanuel Georgiu and Eliza Mardare for all the advice and help, for keeping me company whenever I needed, for being my family while I was abroad.

To my family, my drive-force, the ones who made this work possible, for all the encouragement, patience, advice and support.

To João, for the support, understanding, companionship and love.

To my friends, for listening to me at all times.

Abstract

Protein effect on the corrosion behaviour of titanium modified by two surface treatments

The use of dental implants nowadays has become a regular method to replace missing or awfully damaged teeth.

Titanium is a well known metal used for the construction of orthopedic implants due to its biocompatible characteristics and ability to maintain those while playing the desirable functions. It has the capacity of forming an appealing interface with bone, promoting its growth.

While overcoming some problems related to the functional part of the device, there are still some biological interactions to be studied. By studying the effect of two titanium topographies on the formation of protein layers (mixed layers containing mucin and albumin) as well as the influence of these layers on the corrosion behavior of the surfaces it is expected to get a step forward to understand the interaction between these biologic elements and a dental device.

Electrochemical impedance spectroscopy (EIS) was used to perform the corrosion tests in artificial saliva containing different protein contents.

It was possible to conclude that both proteins had similar resistive behavior, comparing with the control solution (artificial saliva). For the etched samples, neither protein revealed distinct behavior towards the surface; however for the anodized surfaces mucin formed a protein layer evidencing a preference for this surface. When both proteins were in the same solution, it was not detected protein deposition on neither topography.

Resumo

Efeito de proteínas no comportamento à corrosão de titânio modificado com dois tratamentos superficiais

Actualmente, o uso de implantes dentários tem sido método regular para substituir dentes seriamente danificados ou não presentes.

O titânio é um metal conhecido para construção de implantes ortopédicos devido às suas características biocompatíveis e à sua habilidade de as manter enquanto desempenha as funções pretendidas. Tem a capacidade de formar uma interface favorável com o osso, promovendo ainda o crescimento ósseo.

Apesar de superar alguns problemas relacionados com a parte funcional do implante, existem ainda alguns aspectos biológicos a ser estudados. Ao estudar o efeito de duas topografias de titânio na formação de camadas proteicas (camadas mistas de mucina e albumina) bem como a influência destas camadas no comportamento à corrosão destas superfícies, espera-se avançar no sentido de entender as interações entre estes elementos biológicos e os implantes dentários.

Para a parte experimental foi usada a técnica de espectroscopia de impedância electroquímica (EIS) e quatro soluções diferentes, contendo saliva artificial e diferentes constituições proteicas.

Foi possível concluir que ambas as proteínas têm comportamento resistivo semelhante quando comparado com a solução de controlo (saliva artificial). Para as amostras com tratamento superficial etched, nenhuma proteína revelou comportamento distinto; no entanto, a mucina formou uma camada proteica na superfície anodizada, evidenciando dessa forma a preferência por essa topografia. Quando ambas as proteínas se encontravam em solução, não se registou adsorção proteica em nenhuma das superfícies.

Table of contents

Acknowledgements	iii
Abstract	iv
Resumo	v
List of Abbreviations.....	viii
List of Figures	x
List of Tables	xii
Chapter 1 	13
Introduction	13
1.1 Motivation and Objectives	14
1.2 Thesis Organization.....	15
Chapter 2 	16
Related Literature.....	16
2.1 Dental implants: anatomy and causes of failure.....	17
2.2 Titanium in the oral rehabilitation	19
2.2.1 Roughness.....	22
2.2.2 Ion Implantation	23
2.2.3 Wettability.....	23
2.3 Corrosion of titanium in the oral cavity.....	24
2.3.1 Effect of phosphorus and calcium.....	24
2.3.2 Biocorrosion	25
2.3.2.1 Protein influence.....	25
Chapter 3 	28
Materials and Methods	28
3.1 Materials description.....	29
3.1.1 Surface Analysis	29
3.2 Protein and test solutions	31
3.3 Open Circuit Potential (OCP) and Electrochemical Impedance Spectroscopy (EIS) Measurements.....	32
Chapter 4 	34
Results.....	34

4.1 FTIR results	35
4.2 Electrochemical impedance spectroscopy (EIS) results	35
4.2.1 Electrochemical Impedance Spectroscopy (EIS) results for experiments performed on etched samples.....	37
4.2.2 Electrochemical Impedance Spectroscopy (EIS) results for experiments performed on anodized samples	40
4.2.3 Electrolyte Resistance	43
4.2.4 Barrier Film	46
4.2.5 Porous Layer	50
4.2.6 Outer Porous Layer.....	53
4.2.7 Irregular Mucin Layer.....	55
Chapter 5 	57
Conclusions and Future Work	57
References.....	60
Appendix.....	65
Appendix 1.....	66
Tables with the values used for the graphics presented on chapter 4 and respective standard deviation.....	66

List of Abbreviations

ADA	American Dental Association
AS	Artificial Saliva
ASTM	American Society for Testing and Materials
BSA	bovine serum albumin
BSM	bovine serum mucin
C	Carbon
CA	Calcium acetate
CaCl ₂ .2H ₂ O	Calcium dichloride dehydrate
Cl ⁻	chloride ions
cm	centimeter
cpTi	Commercially pure titanium
Da	Dalton
EIS	Electrochemical Impedance Spectroscopy
Fe	Iron
g	grams
h	hour(s)
H	Hydrogen
Hz	Hertz
Ip	Isoelectric Point
KCL	Potassium Chloride
L	Liter
min	minute(s)
ml	milliliter
mV	millivolts
N	Nitrogen
NaCl	Sodium Chloride
NaH ₂ PO ₄ .2H ₂ O	Sodium Dihydrogen Phosphate
Na ₂ S.9H ₂ O	Sodium Sulfate
O	Oxygen
OCP	Open Circuit Potential

Pt	Platinum
Ra	Average Roughness
Rsol	Electrolyte Resistance
SCE	Saturated Calomel Electrode
SD	Standard Deviation
SEM	Scanning Electron Microscopy
Ti	Titanium
TiO ₂	Titanium Dioxide
UM	Universidade do Minho
USA	United States of America
V	Volts
wt%	weight percent
β-GP	β-glycerophosphate

List of Figures

Figure 1 – Implant anatomy: a) comparing with the natural teeth, b) detail of the implant. (10) (11) (12)	17
Figure 2 - Local factors that can affect implant success. [7].....	18
Figure 3 - SEM micrographs of the surface. a) After anodizing treatment. b) Closer look at an anodized Ti surface. c) After etching treatment.....	30
Figure 4 – FTIR spectra for different samples, after 24 hours of immersion on the indicated solutions.	35
Figure 5 – Bode plots for EIS tests performed of etched Ti samples and its evolution with time. Used immersion solution a) AS; b) AS + BSM; c) AS + BSA; d) AS + BSM + BSA.....	37
Figure 6 – Equivalent circuit obtained for the tests performed with etched samples.....	38
Figure 7 - Bode plots for EIS tests performed of anodized Ti samples and its evolution with time. Used immersion solution a) AS; b) AS + BSM; c) AS + BSA; d) AS + BSM + BSA.....	40
Figure 8 - Equivalent circuit model obtained for experiments with the anodized sample immersed in AS, AS + BSA and AS + BSM + BSA.....	42
Figure 9 - Equivalent circuit obtained for the tests performed with anodized samples immersed in AS + BSM.	42
Figure 10 – Electrolyte resistance (R_{sol}) registered for the EIS experiments performed with the etched samples, at different immersion times.	44
Figure 11 – Electrolyte resistance (R_{sol}) registered for the EIS experiments performed with the anodized samples, at different immersion times.....	44
Figure 12 - Barrier film resistance (R_2) registered for the EIS experiments performed with etched samples, at different immersion times.	46
Figure 13 - Barrier film resistance (R_2) registered for the EIS experiments performed with anodized samples, at different immersion times.	46
Figure 14 - Barrier film capacitance (CPE_2) registered for the EIS experiments performed with etched samples, at different immersion times.	47
Figure 15 - Barrier film capacitance (CPE_2) registered for the EIS experiments performed with etched samples, at different immersion times.	48
Figure 16 - Barrier film capacitance (CPE_2) registered for the EIS experiments performed with anodized samples, at different immersion times.....	48

Figure 17 - Porous layer resistance (R1) registered for the EIS experiments performed with etched samples, at different immersion times.	50
Figure 18 - Porous layer resistance (R1) registered for the EIS experiments performed with anodized samples, at different immersion times.	50
Figure 19 - Porous layer capacitance (CPE1) registered for the EIS experiments performed with etched samples, at different immersion times.	51
Figure 20 - Porous layer capacitance (CPE1) registered for the EIS experiments performed with anodized samples, at different immersion times.....	52
Figure 21 - Outer porous layer resistance (R3) registered for the EIS experiments performed with the anodized samples, at different immersion times.....	53
Figure 22 - Outer porous layer capacitance (CPE3) registered for the EIS experiments performed with anodized samples, at different immersion times.	54
Figure 23 - Irregular mucin layer resistance (R4) and capacitance (CPE4) registered for the EIS experiments performed immersing anodized samples in an AS + BSM solution, at different immersion times.	55

List of Tables

Table 1 – Chemical composition for titanium grade 2 (wt %)	20
Table 2 - Mechanical properties for metallic materials.	20
Table 3 - Roughness values.	30
Table 4 - Composition of the Fusayama artificial saliva.	31
Table 5 - Amount of protein added to the Fusayama saliva to produce the protein solutions.	31
Table 6 - pH values for the test solutions.	32
Table 7 – Electrolyte resistance (R_{sol}) registered for the EIS experiments, at different immersion times.	66
Table 8 – Barrier film resistance (R_2) registered for the EIS experiments, at different immersion times.	66
Table 9 - Barrier film capacitance (CPE_2) registered for the EIS experiments, at different immersion times.	67
Table 10 – Porous layer resistance (R_1) registered for the EIS experiments, at different immersion times.	68
Table 11 – Porous layer capacitance (CPE_1) registered for the EIS experiments, at different immersion times.	68
Table 12 – Outer porous layer resistance (R_1) and capacitance (CPE_3) registered for the EIS experiments performed with anodized samples, at different immersion times.	69
Table 13 – Irregular mucin layer resistance (R_4) and capacitance (CPE_4) registered for the EIS experiments performed immersing anodized samples in an AS + BSM solution, at different immersion times.	69

Chapter 1 | Introduction

1.1 Motivation and Objectives

In the USA, statistics show that 69% of the adults with ages between 35 and 44, have lost at least one natural tooth to an accident, gum disease, a failed root canal or tooth decay. By age 74, about 26% of the adults have lost all of their permanent teeth. [1]

Besides the unattractive appearance and the discomfort of eating without one tooth, this problem affects maxillofacial structures in other ways such as the possibility of the adjacent teeth shift and drift, the teeth in the opposite arch extrude into the open space, the bite collapses, the face compresses and sinks inward, the bone of the mandible begins to melt away and the mandible joint function is compromised. [2]

The attempt of replacing missing teeth has been a preoccupation for a few decades. In the last ones, the use of dental implants has increased and improved, being considered nowadays the best solution for this problem, reaching about one million dental implantation per year, worldwide. [1, 2, 3] However, some failures are pointed out such as the degradation of structural materials, adverse biologic reactions and loss of bone material. As titanium is one of the most used materials (comparing with the use of Ti-6Al-4V or Cr-Co-Mo) to produce dental implants, it is important to understand its behaviour in the oral environment [4, 6].

In this case, where bone integration is desirable, the understanding of protein interaction that may lead to the formation of new bone tissue is very important, however not quite understood [5].

The main purposes of the project are:

- To study the effect of 2 different titanium surface treatments on the adsorption and layer formation (mixed layers) by mucin (MUC) and albumin (ALB);
- To analyze the influence of protein layers on the corrosion behaviour of Ti immersed in solutions prepared with Fusayama artificial saliva.

1.2 Thesis Organization

This thesis is organized in 5 Chapters. The present chapter (*Introduction*) is dedicated to introduce the purpose and significance of the study, state the problem and to define the main objectives.

The Chapter 2 (*Related Literature*) constitutes a general introduction, based on literature related to the work that has been developed. This chapter aims to give basic knowledge of the state of the art of the theme.

Chapter 3 (*Materials and Methods*) describes the materials used and the various laboratory methods to prepare the samples, characterize them and perform the experimental tests.

Chapter 4 (*Results*) describes the results and discussion of the research assays accomplished. It is presented the outcome of the experiments, such as graphic data, and the main explanations about its interpretation. This would lead to Chapter 5 (*Conclusions and Future Work*), which comprises a compiled text of the conclusions of the work, as well as some reflections about what could be done to get a more complete study, related to this theme in particular.

The references appear at the end of the thesis document.

Chapter 2 | Related Literature

2.1 Dental implants: anatomy and causes of failure

Dental implants can be defined as non-biologic materials, embedded in the maxilla and/or mandible with the purpose of replacing lost maxillofacial structures. Tooth lost can be a result of trauma, neoplasia and congenital defects (for instance hypodontia). [6, 7]

Throughout time, dental devices experienced shape improvements related to the distribution of forces when applying the implant. The most usual type of dental implant is endosseous comprising a single implant unit (screw- or cylinder-shaped are the most typical forms) placed within a drilled space within the alveolar and/or basal bone. [6, 8, 9]

Nowadays, with an overall success rate of about 90 - 95%, the osseointegration of a dental implant is considered the best treatment for replacing a single tooth. These dental implants are constituted by three components: the implant that is inserted in the mandible; the abutment, which is screwed over the portion of the implant that protrudes from the gum line and provides a surface for the artificial tooth to be placed on; and the crown, which is fitted onto the abutment for a natural appearance and function (Figure 1). [1, ,2, 7]

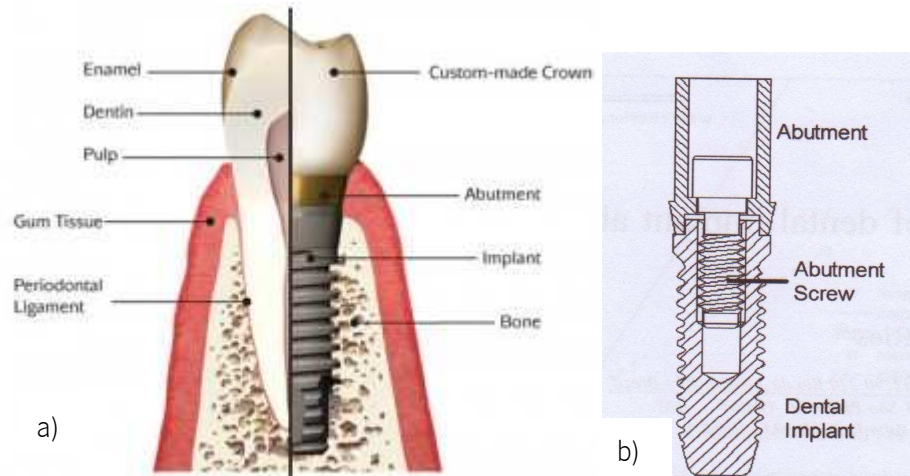


Figure 1 – Implant anatomy: a) comparing with the natural teeth, b) detail of the implant. (10) (11) (12)

It is important to clarify the criteria that to determine an implant success rate. The first ones were proposed by Albrektsson et al (1986): [6]

- The individual unattached implant is immobile when tested clinically;
- No evidence of radiolucency;

- Vertical bone loss must be less than 0,2 mm annually following the implant's first year of service;
- The implant performance must be characterized by absence of signs and symptoms of negative biological reactions such as pain, infections, neuropathies, paresthesia or violation of the mandibular canal;
- Success rates of 85% or higher at the end of 5 years observation period and 80% at the end of a 10 year period (minimum).

In 1989, Smith and Zarb added that the patients and dentist satisfaction with the implant should be considerate, as well as the aesthetic aspect. These criteria have become stricter over the last years, making it difficult to quantify the success rate. [6]

Implant success doesn't depend only on the implant (design and material) but also of some internal factors related to the patient, (see Figure 2) such as bone height, bone density, the amount of attached mucosa, proximity with natural teeth, diabetes, osteoporosis and osteopenia among others. If the first is minimal, it implicates a shorter implant, which has relatively poorer prognosis. Related to the bone density, when placed in dense bone, opposing to spongy bone, the implant's success is higher. [2, 6]

There are also some external factors that can lead to implant failure related to the patient's attitude, like smoking and oral hygiene habits.[1, 13]

Material characteristics
Surface composition and structure
Local temperature
Contaminations
Bone characteristics
Epithelial growth
Loading applied when inserting the implant

Figure 2 - Local factors that can affect implant success. [7]

The choice of the implant type and material used for its construction are crucial to determine the clinical success. The choice of the implant material is related to the term biocompatibility. This does not refer to total inertness of the device, but to the ability of the material to perform its function leading to an appropriate biological response. This characteristic is affected

by the nature of the material, implant design and others. The state of biocompatibility can be referred to a particular time and function in the human body. [2, 6] To determine whether or not the material chosen for the dental implant is suitable for implantation, the American Dental Association draws some parameters: [6]

- a) Evaluation of physical properties to ensure sufficient strength;
- b) Demonstrate the ability of fabrication and sterilization without material degradation;
- c) Evaluation of biocompatibility, including cytotoxicity tests;
- d) Lack of defects;
- e) Perform at least two clinical trials, conducted for 3 years to get provisional acceptance or 5 years for acceptance, each trial with 50 human subject minimum.

The good acceptance of orthopedic and dental implants in particular is related to bone interaction. Branemark *et al.* (1977) studied osseointegration (or osteointegration) to understand better the needs of the material's surface to be incorporated into natural bone. This concept describes the direct bone-to-implant interface at the optical microscopy limits (0.5 μm), without any fibrous tissue growing at this interface. [9, 14] The material used to construct any biologic implant must be biocompatible, promote osseointegration, not cause adverse biological reaction, be stable and maintain its functional properties. [15] This type of guide lines are important to assure that the material can perform its function without trigger any defense mechanism from the human body, since in this case it could cause pain and ultimately lead to the total removal of the implant. [1, 9]

2.2 Titanium in the oral rehabilitation

Commercially pure titanium (cpTi) is the most popular material used for implants in medicine, including dental implants. [8, 9, 16] It is a natural element, composing about 0.6 % of the earth crust, a million times more abundant than gold and represented in the periodic table by the number 22. There are a few grades of titanium, depending on the interstitial elements quantity: the higher the grade, higher the impurities percentage. Titanium grade 2 has 99.6 purity percentage and its components are presented on Table 1.

Table 1 – Chemical composition for titanium grade 2 (wt %).¹

Titanium	N	C	H	Fe	O
CP grade II	0.03	0.08	0.015	0.3	0.25

Titanium is used for oral implants due to its advantageous properties, like high heat resistance, high strength, high resistance to corrosion, low density and good biocompatibility (in particular with human hard tissue). [16, 17] Table 2 presents some characteristics of titanium, along with the comparison with other materials. [18]

Table 2 - Mechanical properties for metallic materials.

Material	Grade/ Condition	Yield Strength (MPa)	Elongation (%)	Elasticity Modulus (GPa)	Tensile strength (MPa)	Density (g/cm ³)
CP Titanium	2	275	20	102	345	4.5
Ti-6Al-4V	—	860	10	113	930	4.4
Co-Cr-Mo	Cast	450	8	240	700	8.0
Stainless Steel	Annealed	190	40	200	490	8.0
	Cold-Worked	690	12	200	860	8.0

This material is also characterized by its capacity of adsorb molecules and incorporate elements. [19, 20] This characteristic is guaranteed by the thin oxide layer formed spontaneously on the surface. [6, 9, 15] However, the layer formed in open air is not effective in improving the bioactivity of the titanium implants due to its small thickness [21]. It has three varieties: TiO, TiO₂ and Ti₂O₃. In a natural atmosphere, the second one (TiO₂) is thermodynamically stable, therefore more common. [19, 22, 23] Its physico-chemical and electrochemical properties allied to its long-term stability in biological environments is very important for titanium implants biocompatibility. [15] TiO₂ exists in three different crystalline structures: anatase (tetragonal), rutile (tetragonal) and brookite (orthorhombic). Anatase is the low-temperature form of this oxide and can be obtained just by anodization. [20, 22, 24, 25] Despite its biocompatibility, this layer reacts with nonorganic ions,

¹ Based on the USA ASTM Grades for ASTM B265.

water and other species existing in physiological fluids. It has been reported that this layer triggers the precipitation on calcium ions existing in biological fluids, increasing its biocompatibility. [16]

Even though being made of a bioinert metallic material, titanium implants cannot bond to living bone directly nor induce bone growth directly. Therefore, implants have to suffer surface modifications until be suitable for implantation, in an attempt to improve its bioactive-bonding ability, biological responses that occur during osteointegration and the long-term response of bone-implant interface. [14, 17, 23, 26] These modifications can combine passivation, ion implantation and texturing. [21, 27]

The texturing, which can be achieved through acid etching, increases the surface area of the implant up to 6 times. This enhances osseointegration making more room for the bone to contact and bond with the implant. [6, 7, 9, 14] This can reduce healing times and accelerate integration into the host tissue. In the case of orthopedic implants, this type of topography modifications can improve the mechanical adhesion to bone and the asperities and grooves may become preferable sites for protein adsorption. [14]

Passivation implies the growing of the oxide layer on its surface to prevent the release of metallic ions from it, thus enhancing biocompatibility. These treatments can be made through anodization (anodic oxidation), where an electric current is passed through the metal, making the oxide layer thicker, improving corrosion resistance. Yang et al. (2004) reported that the bioactivity of the titanium implant is more related to the surface roughness than to its crystalline structure. [23] The composition, structure and thickness of total oxide film determine its stability. Indeed, studies indicate that the thicker the oxide film, the higher the capacity of reducing the passivity current in physiological solutions. Thus, preventing ion release and dissolution of titanium in biological environment, which can change the environmental fluid conditions and influence the response to the implant. [19] The morphology of the surface and the thickness of this oxide layer depend on the method applied for its formation and it influences the interaction of the implant with the biological environment. Sul et al. indicated that the behavior of the oxide film developed electrochemically depends on the anodic parameters such as the electrolyte concentration, the applied current density, the anodic forming voltage, the given temperature, the agitation speed and the surface area ratios of cathode to anode. Kuromoto et al. (2007) concluded that the thickness of the oxide film increased with the applied voltage. [22] The film produced electrochemically, depending on the

applied voltage, can be composed by two layers: the inner Ti oxide layer (composed by anatase crystals) and the outer Ti porous oxide layer formed at the film/electrolyte interface. [17, 19, 22]

According to Le Guéhennec et al. (2007) anodized surfaces lead to a strong reinforcement of the bone response, greater values for biomechanical and histomorphometric tests, when comparing to machined surfaces. [3]

However, chemical treatments can also influence the mechanical characteristics of titanium. According to Guéhennec et al. (2007), acid-etching can lead to hydrogen embrittlement of the titanium, creating micro-cracks on the surface that can reduce fatigue resistance of the implant. The adsorption of hydrogen by titanium in biological environments can also lead to hydrogen embrittlement with the formation of a brittle hybrid phase which reduces the ductility of titanium. Fracture mechanisms in dental implants are related to this phenomenon. [3]

2.2.1 Roughness

Surface roughness of dental implants is a very important aspect since it affects the rate of osseointegration and biomechanical fixation. Rough surfaces have demonstrated superior outcome in cases when there is insufficient quality or volume of the host bone.[14, 26]

This characteristic can be divided in macro-, micro- and nano-sized topologies. The macro level is in the range of millimeters to dozens of microns. This level of roughness can improve the early fixation and long-term mechanical stability since it results in mechanical interlocking between the implant and bone ongrowth; however it may increase peri-implantitis and ionic release. The micro level is in the range of 1 to 10 μm , it maximizes the interlocking mentioned before. Implants with this level of roughness demonstrated greater bone-to-implant contact and higher resistance to torque removal comparing to other topographies. The nanometer range plays an important role for protein adsorption despite it is not known the optimal nano topography. However it is difficult to produce reproducible surfaces at this level with chemical treatments. [3, 14]

Aparicio et al. (2011) tested acid-etching surface modification (in 0.35 M hydrofluoric acid for 15 s at room temperature) on titanium grade III. The results showed that the experimented treatment accelerate bone tissue regeneration and increased mechanical retention comparing with other implants tested. Roughness values of $R_a \approx 4.5 \mu\text{m}$ favored osseointegration at short- and mid-term healing. [22, 26]

It has also been reported that increased roughness can cause an increase in calcium and phosphorus depositions after immersion in artificial biological solutions, higher protein production and calcium up-take in osteoblasts-like cells. Porous and rough titanium surfaces have been suggested to cause microscopic tissue-cell ingrowth, improving implant fixation. Pores should have at least 100 μm in diameter, which does not exclude roughness in the micron- and nanometric scale. [19]

2.2.2 Ion Implantation

With ion implantation it is possible to attach ion into the superficial layer of the material. According to Zhu et al. (2001) implants have the ability to bond directly to the bone if their surface provides reactive silica, calcium and phosphate groups in an alkaline environment. The surface containing Ca and/or P leads to osteoinduction of new bone and it also becomes bioactive. This can be obtained by developing the oxide film by anodizing titanium and implanting Ca and P through the electrolyte of β -Glycerophosphate (β -GP) sodium and calcium acetate. Smoother surfaces are more likely to induct the formation of thicker fibrous encapsulation than those with rougher surfaces. [19]

2.2.3 Wettability

. Biomolecule adsorption onto implant surfaces in vivo is a dynamic process driven by physico-chemical interactions between the adsorbent surface and the macromolecules. As a consequence, wettability is an important parameter to have into account when considering protein adsorption. Fibrin adhesion, promoted by hydrophilic surfaces, provides contact guidance for the osteoblasts migrating along the surface. [3] As the topographies used in this project are considered hydrophilic, it is considered the possibility of being accepted by the host tissue and favorable to bone attachment.

Wettability can be described as the affinity of a solid surface to be wetted by a given liquid (usually water) and it is strongly influenced by surface roughness. Hydrophobic surfaces (i.e. surfaces with low water wettability) are assumed to decelerate primary interactions with the aqueous biosystem. It has been reported that hydrophilic surfaces (contact angles from 0° to 140°) improve the interaction with body fluids and cell growth. [14, 21]

2.3 Corrosion of titanium in the oral cavity

Corrosion can be defined as a set of electrochemical reactions between a material and its environment that produces an alteration on its properties. These reactions follow the laws of thermodynamics, being time and temperature dependent. When immersed in an electrolytic solution, metals generate at least a pair of reactions: the oxidation of the metal ($M \rightarrow M^{n+} + ne^-$) and the reduction of hydrogen, along with the dissolution of oxygen, generating water molecules ($O_2 + 4H^+ + 4e^- \rightarrow 2H_2O$). [25, 28, 29]

For oral rehabilitation, corrosion is an important parameter to any metal used for the implant since it can adversely affect biocompatibility and mechanical integrity of the device. Allied to surface film dissolution, these are the two main mechanisms able to introduce additional ions to the body. The release of metallic ions from any prosthetic device can result in adverse biological reactions and can lead to its mechanical failure. [15, 30, 31, 32]

There are several factors that affect corrosion in the oral cavity, the most noticeable is the one induced by the aqueous environment, due to the presence of ions, such as Cl^- , H^+ sulfide compounds (S^{2-}), dissolved oxygen (O_2), and biological media, such as microorganisms and other biologic material, in the human saliva. [30, 33] Concerning titanium dental implants, the upper part of the implant and the abutment are specially exposed to these elements since they protrude from the gum tissue.

The periodical presence of food, drinks and toothpastes also induces alterations on the area surrounding the dental zone, like changes in pH values. This parameter influences not only the oxide film of an eventual existing implant, but also interfere with protein deposition on the surface of the material. [34]

The body temperature is also said to accelerate electrochemical reactions and sometimes change the mechanism of corrosion from the one that would occur at room temperature. [35]

2.3.1 Effect of phosphorus and calcium

The spontaneous formation of calcium phosphate can be accelerated when the metal surface is modified with ion implantation, previous to its use. Calcium and phosphate are the most common mineral ions to be incorporated since they occur naturally in the human bone. [3, 36] Hanawa et al. reported the use of calcium ions for the implantation to accelerate the precipitation of

calcium phosphates (primary inorganic phases of hard tissues), being advantageous for the growth of bone tissue and demonstrating osteoinductive properties in physiological solutions. [19, 37] They also found that with this implantation, the thickness of the oxide layer increased, forming CaTiO_3 , since it's mixed with the titanium oxide layer. [9, 16]

Krupta et al. (2001) suggested that the implantation of calcium and phosphate into the surface of titanium would increase its polarization resistance under stationary conditions. The same study confirmed the biocompatibility of calcium-implanted titanium, since cell cultures behave equivalently for calcium-implanted titanium surface and for the control sample (the bottom of the culture dish). [16]

2.3.2 Biocorrosion

The fluid present in the oral cavity, also known as “whole saliva”, “mixed saliva” and “oral fluid” is composed by water (99.5%), proteins (around 0.3%), such as mucins, and traces of inorganic substances (0.2%). Biochemically, proteins are the most important constituents of saliva, they are mostly glycoproteins, enzymes, immunoglobulins and peptides with antimicrobial activities. The inorganic part of saliva contains electrolytes (sodium, potassium, chloride and bicarbonate) that also exist in other body fluids in different concentrations. [33, 38]

The amount and composition of secreted saliva depends on several factors, for instance age, gender, blood type, diet, drugs. It can achieve from 0.3 up to 7 mL per minute with about 0.5-1.5 L per day. Saliva pH can range from 6.2 to 7.4, although, when it arrives to the oral cavity it becomes a little acid due to the presence of external elements (such as traces of food) and microorganisms. [33]

Standardization of saliva is important when it is used as a research material, since saliva composition varies greatly both intra- and inter- individuals. [33] There are various types of artificial saliva, such as the Fusayama artificial saliva, that attempt to simulate the inorganic part of the natural saliva.

2.3.2.1 Protein influence

Interaction of proteins and cells with biomaterials dictates the clinical success of implant devices. In the oral environment, these interactions are desirable, since integration onto the bone is

needed. [5] Proteins are biomolecules that have the tendency to accumulate in the interface of the solution and solid surfaces. [39, 40] This adsorption occurs whenever the proteins in solution become in contact with a solid surface. It can even reduce the corrosion rate: the adsorption of proteins may limit the diffusion of oxygen to some regions of the surface. [35] On the other hand, there are also studies that report dissolution enhancement due to the formation of metal ions and protein complexes. However, it is still not clear whether biomolecules accelerate or inhibit electrochemical reactions on titanium surfaces. [35, 41]

Mucins are large glycoproteins ($>10^6$ Da), known for its adsorption and lubricant abilities. It exists in the oral cavity and has the ability of forming thick and highly hydrated films when in solid/liquid interaction. [41, 42, 43] These films end up protecting the material they are adsorbed to, although microorganisms can proliferate on them.

It has been reported that bovine serum mucin (BSM), forms extensive layers on negatively charged hydrophilic surfaces. [42] The adsorbed mucin layer depends on the mucin source, solution conditions and type of substrate (non-polar, polar and polar-charged). [41, 42]

According to Lundin et al. (2009), it has been shown that other proteins, such as albumin, associate naturally with mucin. [42]

Albumin is the most abundant protein present in blood plasma (around 40 g/L), therefore, its influence is widely studied for application of implant devices, although it is not quite understood its structure when adsorbed onto titanium, with or without other proteins in solution. It has a molecular weight of 66.5 kDa. [5, 39, 40, 41, 42] Because of its naturally high concentration this protein arrives first at the implant surface, playing an important role in the initiation of protein adsorption onto biomedical surfaces. [39, 44]

Protein adsorption is highly influenced by the solution pH. It is widely known that when the pH is around the protein's isoelectric point (IEP - value of pH at which the protein activity is improved), its adsorption is enhanced, since the electrostatic interactions between the protein and the implant surface are minimized. [5] According to Jansson et al. (2004), a pH value close to the protein's IEP decreases the overall charge of the protein molecule and its degree of hydration, allowing short-range attractive forces and hydrophobic interactions to take place. They also verified that albumin deposition is more significant in porous hydrophilic surfaces [5, 45, 46]

Mucin's IEP is 3, but its appropriate adsorption behaviour has been verified in a pH range of 3 up to 7.4 [41]. The IEP of albumin is around 4.9. [44, 45]

When these proteins come together, it is expected mixed protein layers to be formed on the titanium surfaces after immersion. According to Lundin et al. (2009), who studied the adsorption kinetics of BSM and BSA in mica, the adsorbed amount of BSA is independent of the concentration of BSM in solution; in contrast, the higher the concentration of BSA in the solution results in reduced amounts of adsorbed BSM. Also, in these studies, the amount of adsorbed material was higher when both proteins were present in the solution than when there was only BSA, which may indicate that both proteins adsorb to mica, forming mixed layers. [42]

Chapter 3 | Materials and Methods

3.1 Materials description

Titanium specimens were cut in 20 x 20 x 2 (\pm 1 mm) of dimension, from a sheet of commercially available pure titanium (cpTi grade 2, Goodfellow Cambridge Limited, England) and then prepared with different treatments: anodized and etched. The etched treatment was also used as a way to standardize surface characteristics, so that the tests could be performed in homogeneous surfaces.

The etched specimens were obtained by immersing the cpTi samples in Kroll's reagent (2 ml HF, 10 ml HNO₃ and 88 ml H₂O) for 10 minutes. Then they were immersed in distilled water at 60° C in ultrasound, to stop the effect of the acid. Some samples were cleaned and stored, while others proceeded to the anodize treatment.

The standard cleaning process consists of several steps: 10 min immersed in ethanol followed by 5 min immersed in acetone, both times in ultrasonic bath. Then they were individually dried with a cold air blow drier and bagged.

The anodized surfaces were obtained by immersing, individually, etched samples in 200 mL of a solution containing 0.7 mol/L of calcium acetate and 0.04 mol/L of β -glycerophosphate, and submitted at 300 V for 1 min. The oxide film of these specimens is complex and it's expected to have about 4 μ m thick.

3.1.1 Surface Analysis

For surface analysis some optical tests were performed to evaluate the surface composition and to access the existence of a protein layer.

Scanning electron microscopy (SEM) is a well known technique for surface imaging and it is a simple way of getting an insight about the surface. [14] It was used to analyse the surface structure, as shown in Figure 3.

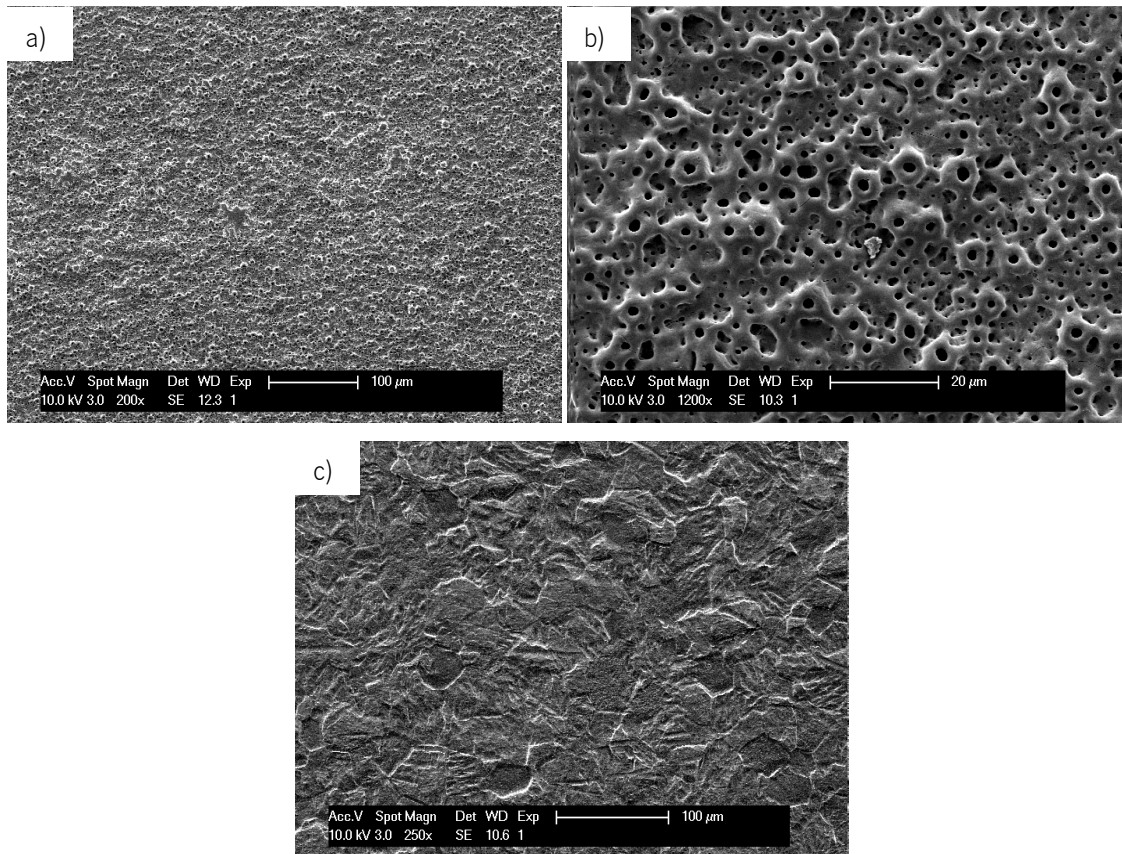


Figure 3 - SEM micrographs of the surface. a) After anodizing treatment. b) Closer look at an anodized Ti surface. c) After etching treatment.

Anodized surface presents pores, in the Figure 3 b) there is also evidence of pores with various depths and sizes. The surface of the material is enhanced, which could be valuable for protein adsorption.

For the reasons already stated in Chapter 2 (*Related Literature*), there was the necessity to access the roughness of the test samples by a profilometer method (instrument Mahr, S5P).

Table 3 - Roughness values.

Samples	Ra ± SD (μm)
Etched	0.56±0.0597
Anodized	0.79±0.0713

From the values of Table 3, one can estimate that anodized samples have higher roughness values, being theoretically better for protein adsorption. This was already expected from

the SEM images, since the anodized samples presented pores and the etched ones seemed smoother.

Fourier transform infrared (FTIR) spectroscopy allows to detect functional groups in molecules on a surface [48] by obtaining an infrared spectrum of absorption. The spectrum or scattering can be obtained for solid, liquid or gas surfaces. It can be performed using a spectrum of wavenumbers taken from an infrared range (4000 to 800 cm^{-1}). The tests were performed with FT-IR Perkin Elmer 2000 spectrometer, the spectral acquisition 100 scans, resolution 4cm^{-1} .

3.2 Protein and test solutions

It was chosen 4 test solutions for the electrochemical tests: Fusayama artificial saliva (AS), as the control/blank solution; a mixture of AS and mucin (AS + BSM); a mixture of AS and albumin (AS + BSA); and a mix solution using AS and both protein simultaneously (AS + BSM + BSA). All of the test solutions were produced 24 hours before the tests, so that they were homogeneously mixed. The quantities of the elements used to produce these solutions are described on Tables 4 and 5.

Table 4 - Composition of the Fusayama artificial saliva.

Compound	Concentration (g/L)
NaCl	0.4
KCl	0.4
CaCl ₂ .2H ₂ O	0.795
Na ₂ S.9H ₂ O	0.005
NaH ₂ PO ₄ .2H ₂ O	0.69
Urea	1

Table 5 - Amount of protein added to the Fusayama saliva to produce the protein solutions.

Protein	Concentration (g/L)
Mucin	1.4
Albumin	4

It was used 1.4 g/L of mucin (bovine serum mucin – BSM), since it is the medium concentration of this protein in the oral cavity, and 4 g/L of albumin (bovine serum albumin – BSA) [(34), (41), (49)].

As stated previously, protein adsorption is highly influenced by the solution pH (see Table 6).

Table 6 - pH values for the test solutions.

	Artificial Saliva	Artificial Saliva + Mucin	Artificial Saliva + Albumin	AS + BSM + BSA
	4,94	6,73	6,00	5,23
	4,84	6,84	6,04	5,24
	4,92	6,88	6,04	5,20
	5,17	6,75	5,50	5,21
Average	4,97	6,8	5,9	5,2

Despite the Ip of mucin be around 3, the adsorption is not affected in the range of pH 3 until 7.4 [41]. The Ip of albumin is around 4.9 and the values of pH presented above are around those values, there shouldn't be significant changes in the adsorption property of this protein. [35, 50].

3.3 Open Circuit Potential (OCP) and Electrochemical Impedance Spectroscopy (EIS) Measurements

The tests alternate 1 hour of OCP followed by electrochemical impedance spectroscopy (EIS). This was performed by superimposing a sinusoidal signal of 10 mV on the signal of the stable value of OCP. Measurements began at 10^5 Hz and terminated at 10^2 Hz, with a frequency sweep of 5 frequencies/decade. For each sample, this sequence was completed 6 times, consecutive and continuously, up to 9 hours of immersion time.

Hopefully, these tests will serve the purpose of acquiring information about the degradation behaviour of the material, in presence or absence of these proteins [51] and allow to estimate the value of the materials resistance to corrosion in the immersion solution. With the impedance response in the Nyquist or Bode format it may be easier to understand the processes that happen on the surface with the adsorbed proteins [49, 50, 52].

It was used a Gamry Reference 600 potentiostat, the reference electrode was a saturated calomel electrode (SCE); the working electrode was the Ti specimen with a working area of 0.38 cm² and the counter electrode a platinum (Pt) electrode.

All the tests were performed in a 37 °C (physiological temperature) distillate water bath where the electrolyte cells were filled with 200 mL of the respective solution, simulating the oral environment. The surrounding ambient air would have around 50% RH and 23 °C.

The whole system was covered to prevent light from degrading the proteins and influence the measurements, keeping the same conditions is every test.

It was performed at least 3 tests for each condition for reproducibility purposes.

Chapter 4 | Results

4.1 FTIR results

On the graphic of Figure 4 are presented the results obtained by the infrared Fourier method, for all test samples.

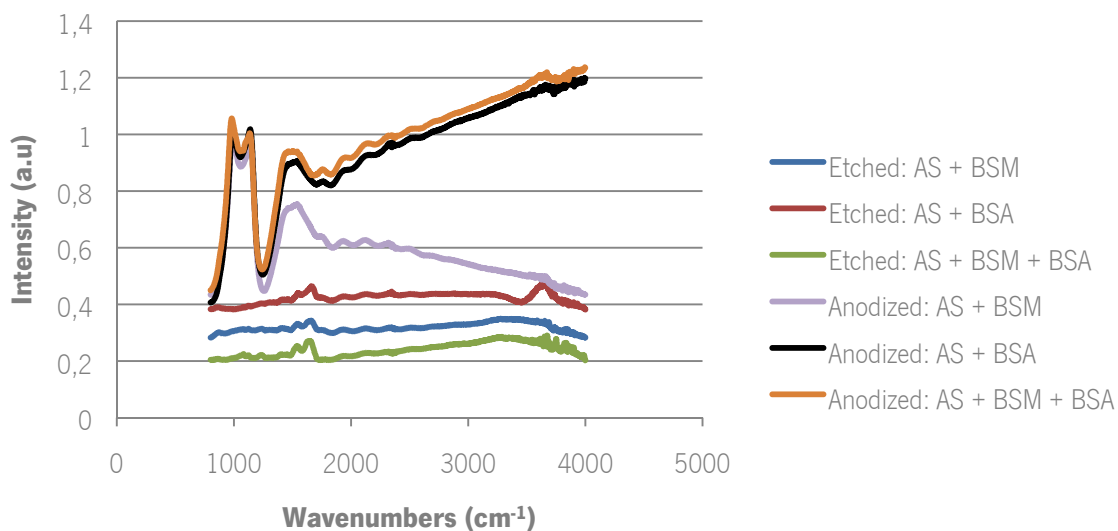


Figure 4 – FTIR spectra for different samples, after 24 hours of immersion on the indicated solutions.

For all test samples, the peak around 1040 to 1120 cm^{-1} may indicate the presence of mucin on the surface of the sample. In the case of the etched samples, the first peaks (around 1500 and 1600 cm^{-1}) reflect the existence of proteins (evidenced by the presence of amide I and II). Since the surface of etched and anodized samples are very different, with only this analysis it is not possible to conclude about which surface is more suitable for adsorption. [47, 48]

4.2 Electrochemical impedance spectroscopy (EIS) results

Comparing the EIS results obtained from the tests using only AS with the ones obtained when using proteins in the immersion solution, one can hope to conclude about the influence of the presence of proteins. On the other hand, since it was made the same tests on samples with different surface treatments, one can also attempt to infer about the influence of these two topographies in the protein adsorption.

In Figures 5 and 7, Bode spectra are presented. These consist on two diagrams on one graphic, showing the magnitude of the impedance ($|Z|$) versus the frequency (f), on a logarithmic scale, and a phase angle (Φ), against the log frequency. These diagrams allow to easily obtain information about changes that may occur in the working electrode surface. [58, 60]

On the Bode diagrams presented in this chapter the scattered lines represent the Bode impedance modulus and the ones with the solid symbols represent the phase angles, both versus frequency. The several curves of each diagram represent the evolution with time of the Impedance Modulus *vs.* Frequency and Phase Angle *vs.* Frequency.

The obtained Bode diagrams were fitted to electrochemical equivalent circuits. Satisfactory fitting results were obtained for all the EIS data with chi-square values ranging 5×10^{-4} to 1×10^{-3} .

4.2.1 Electrochemical Impedance Spectroscopy (EIS) results for experiments performed on etched samples

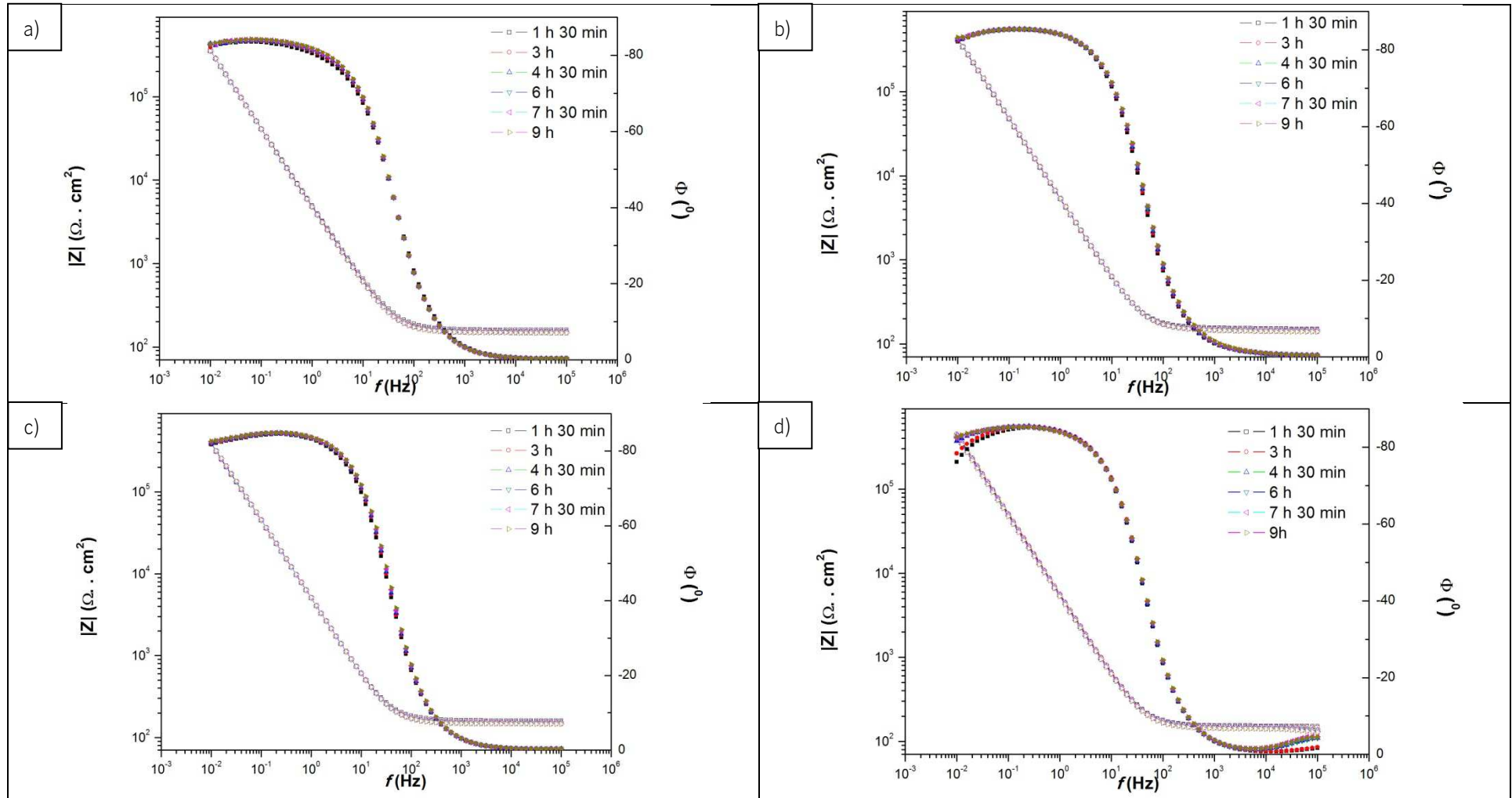


Figure 5 - Bode plots for EIS tests performed of etched Ti samples and its evolution with time. Used immersion solution a) AS; b) AS + BSM; c) AS + BSA; d) AS + BSM + BSA.

Figure 5 presents examples of Bode plots obtained for etched samples immersed in the respective fluid. Commonly to all pictures from the figure (a), b), c) and d)) the evolution of the Impedance Modulus ν s. Frequency reveals a plateau at the high frequencies region. With a phase angle close to 0° , it is possible to read, in the impedance axis, the value of the electrolyte (or solution) resistance (R_{sol}).

As we go to lower frequencies, there is a near-capacitive behavior illustrated by a phase angle close to -90° over a wide frequency range (from 1 to 0.01 Hz) associated with the negative slope of the impedance curves. At this point it is possible to assume that there is a constant phase element represented in this region, which might indicate the existence of a protective film on the surface of the material, whatever the immersion solution was. [53] In this region it is also possible to infer about the high value of the total resistance, that is the sum of the polarization resistance (R_2) with the electrolyte resistance. [54] The value of the polarization resistance alone can be obtained at the lowest frequency. It can indicate that there is a stable protective film on the surface of the material. [54]

Regarding the evolution with the increasing time of immersion, for all the samples there are no significant visible changes. In picture d), where the immersion solution uses both proteins, it is possible to observe that the polarization resistance increases with time, but not significantly to assume that it is due to the deposition of protein in the surface of the electrode.

As the scale of all diagrams is the same (for comparison purposes), it is possible to state that the behavior of the etched samples is similar, regardless the immersion solution.

Adjusting the presented diagrams to an electrochemical equivalent circuit it was obtained the circuit schematized in Figure 6.

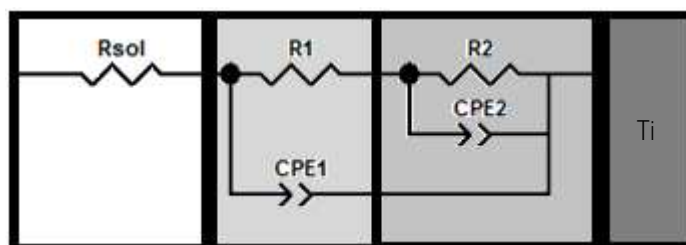


Figure 6 – Equivalent circuit obtained for the tests performed with etched samples.

In this scheme, R_{sol} represents the solution resistivity, also known as electrolyte resistance; R_1 is an additional resistance that, copulated with CPE_1 , may be referred to a porous or non-

regular surface. The resistance represents the resistive behavior of the solutions in the pores or between asperities and the constant phase element represents the effect of the film material in this layer. The pair R2 and CPE2 represents the native oxide film that is naturally formed in the titanium surface.

Although in the Bode diagrams it is only visible one constant phase element, it is possible that there is a light inflection of the impedance curve that indicates a second CPE, as the simulation evidences.

This equivalent circuit was also suggested for experiments with a consolidated silver dental biomaterial, immersed in Fusayama artificial saliva. [50]

4.2.2 Electrochemical Impedance Spectroscopy (EIS) results for experiments performed on anodized samples

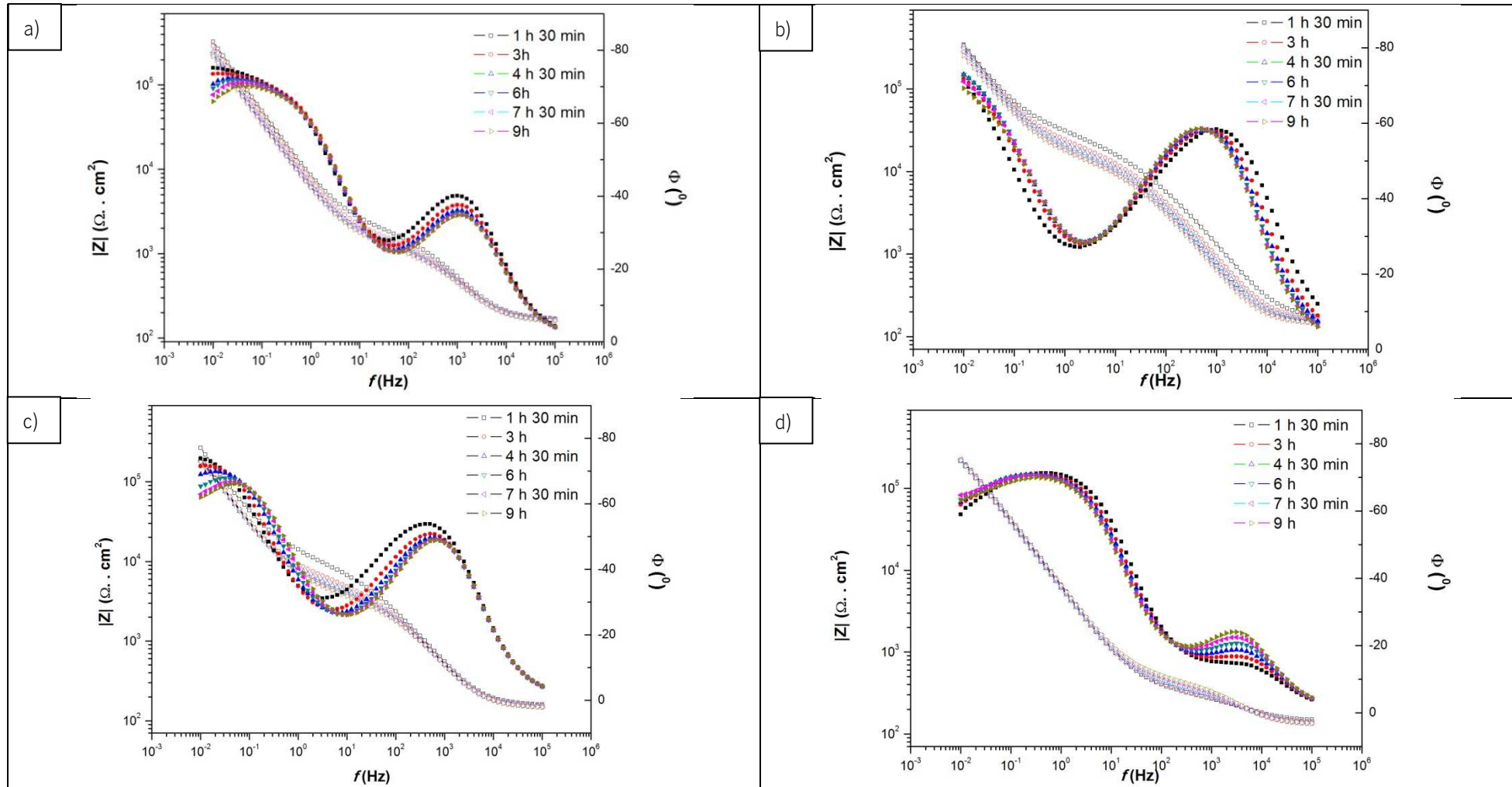


Figure 7 - Bode plots for EIS tests performed of anodized Ti samples and its evolution with time. Used immersion solution a) AS; b) AS + BSM; c) AS + BSA; d) AS + BSM + BSA.

At first sight it is immediately visible that the behavior of these samples is distinct from the verified earlier with the etched samples, and that the immersion solution seems to influence the behavior of these samples.

For all diagrams of Figure 7 it is common that in the high frequency region it is barely understood a resistive behavior related to the electrolyte resistance (R_{sol}), since a stable plateau is absent on the impedance modulus curve. Also, in all diagrams it is visible that possibly there might be two constant-phase elements, indicated by the two peaks on the phase angle curve along with the negative slope of the impedance modulus curve. They might be explained by the presence of a two layer oxide film on the surface. [55, 56]

At intermediate frequencies, the phase angle curve doesn't cover a wide frequency range; it can be acknowledged that the passive film is not as stable as the one in the etched samples or that the composition of this first layer is different. Since it is known that this surface treatment provides a porous surface, it is possible to deduce that this first near-capacitive behavior is due to the pores on the surface. The solution penetrates into the pores, therefore it doesn't offer many resistance to the current passage (according to its impedance value). Comparing all the diagrams it is possible to conclude that the highest impedance modulus is presented from the samples immersed in AS + BSM, and the lower value found for this parameter corresponds to samples immersed in the mixed solution. It may be caused by protein interference or pH difference.

In Figure 7, near the lower frequencies region, there is a second elevation on the phase angle curve (angle around 80°) along with a higher impedance value. It might represent a second layer with more stable characteristics (compact, less porous or with different porous characteristics). In a), c) and d), there is in fact a small plateau, (more evident in a)) which might indicate an increasing stability.

The absence of a well defined plateau in the low frequencies regions might indicate that the film on the surface of the anodized samples is not as stable as the one on the etched electrodes.

The value of the polarization resistance (R_2) can be obtained from the impedance curve at the lowest frequency (around $2 \times 10^5 \Omega \cdot \text{cm}^2$). Comparing with the ones from Figure 5, these R_2 values are much smaller, indicating a different surface, possibly less resistive.

Regarding the evolution with time, the impedance values decrease slightly for each sequence of testing. It appears that the continuous immersion decreases a little the resistance of the immediate passive film of the surface. It can indicate that the surface suffers modifications possibly due to the adsorption of the protein in solution, or that the increasing immersion time

allows the solutions to interpenetrate into the pores and, as a consequence, the current passes through the solution ions present inside de pores. [39]

The fitting performed by adjusting these diagrams to an electrochemical equivalent circuit resulted in the circuit schematized in Figure 8 and Figure 9.

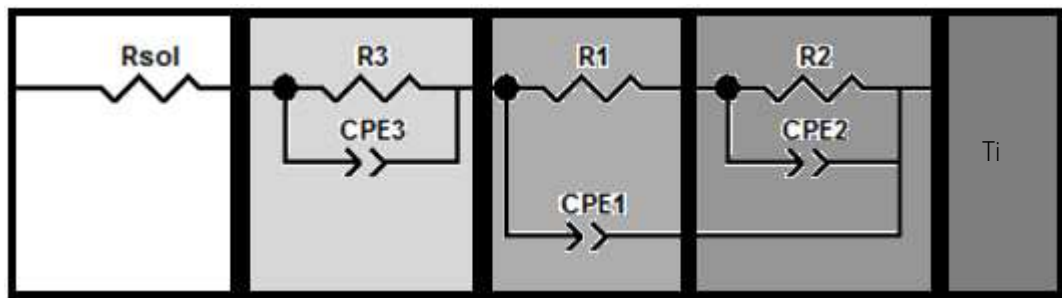


Figure 8 - Equivalent circuit model obtained for experiments with the anodized sample immersed in AS, AS + BSA and AS + BSM + BSA.

The proposed circuit from Figure 8 was also suggested by Ibris et al. when working with titanium anodized samples, although immersed in Hank's solution. (55)

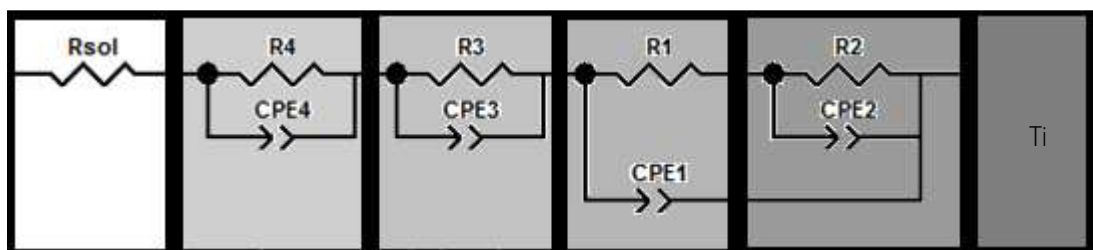


Figure 9 - Equivalent circuit obtained for the tests performed with anodized samples immersed in AS + BSM.

Some components are common to the circuit model obtained for the etched samples. R_{sol} represents the solution resistivity; R_1 and CPE_1 represent a porous surface; and R_2 and CPE_2 represent the native oxide film that is formed in the titanium surface.

The parallel pair R_3/CPE_3 represents the outer porous layer, being the resistance representative of the resistive behavior of the solution in the pores and the constant phase element representative of the capacitive effect on the oxide material. For the circuit model obtained for the samples immersed in AS + BSM, R_4 and CPE_4 , might correspond to an irregular protein layer, that adsorbs to the surface of the material.

Although in the Bode diagrams it is only visible two constant phase elements, it is possible there could be other inflections of the impedance curve that indicates the others CPE, as the simulations support.

Comparing this equivalent circuit with the one obtained for the tests with etched samples, the mucin layer appears to have greater influence on the anodized specimens.

Comparing the diagrams from Figure 6 with the ones from Figure 8 there are noticeable differences, starting with the absence, in the first ones, of the two layer protective film, revealed by the two constant phase elements. It was already expected, since others works were performed with anodized treatments, and revealed the duplex structure of the formed film: a thinner, compact and less porous inner layer and a thicker and more porous outer layer. [55]

The porous surface influence of the proteins seems to have much more significance effect on the proteins ability to adsorb since the curves of the impedance modulus and of the phase angle are different from the ones obtained when using the etched surfaces.

The fitting allowed the calculations of the circuits' components that may simulate the electrochemical behavior of the titanium specimens. The values for these components, obtained for each immersion time, are presented on the following subchapters.

4.2.3 Electrolyte Resistance

The influence of the immersion time in R_{sol} throughout the EIS tests is present on Figures 10 and 11, for the 4 test solutions and the 2 types of samples used in the experiments. The values for the standard deviation are between $1,9 \times 10^{-4}$ and 9×10^{-3} .

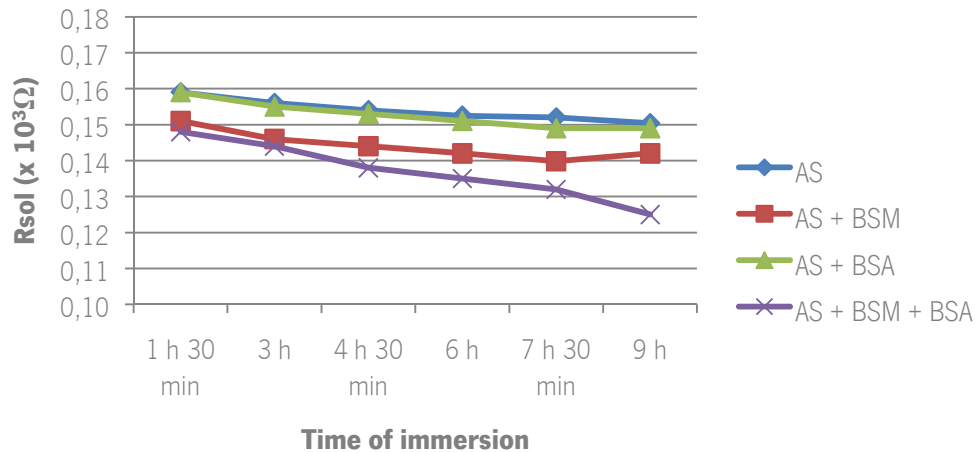


Figure 10 – Electrolyte resistance (R_{sol}) registered for the EIS experiments performed with the etched samples, at different immersion times.

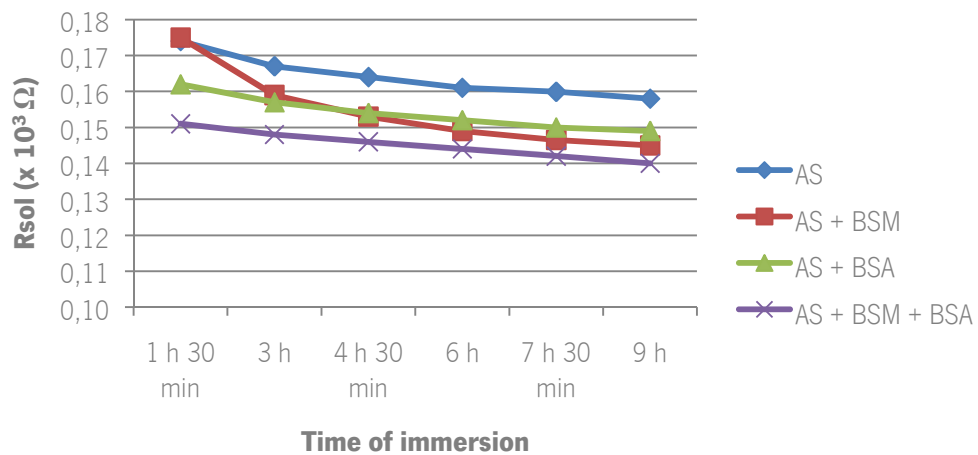


Figure 11 – Electrolyte resistance (R_{sol}) registered for the EIS experiments performed with the anodized samples, at different immersion times.

At first sight, it is possible to notice that the resistive behavior of the electrolyte decreases throughout the immersion time, for all test conditions.

In the EIS experiments with the control solution, the value of R_{sol} is higher than for all the other test solutions. This indicates that this solution offers difficulty for the current to pass. Therefore, judging only by these values, the proteins appear to facilitate the corrosion process.

Comparing the resistive behavior of the solutions containing proteins, the mixture of proteins appears to decrease the electrolyte resistance, presenting the smallest value of R_{sol} . The interaction between both proteins appears to facilitate the transfer of energy.

For the same immersion solution and comparing between the different samples, Rsol presents slightly higher values for tests performed with the anodized specimens. However the differences are not significant enough to take any conclusion.

4.2.4 Barrier Film

The barrier film is represented in the equivalent circuits by R2 and CPE2. Since it refers to the natural film formed on the titanium surface, the values obtained for the fitting for each EIS test are comparable between test samples and presented on the following diagrams (Figures 12, 13, 15 and 16). The values for the standard deviation for the values of R2 are between 0,0153 and 3,39; for the values of CPE2 are between 0,247 and 4.

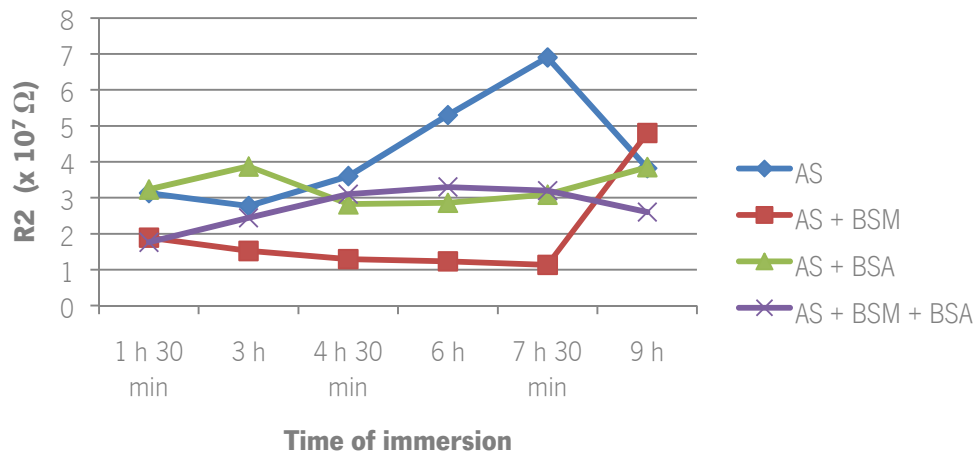


Figure 12 - Barrier film resistance (R2) registered for the EIS experiments performed with etched samples, at different immersion times.

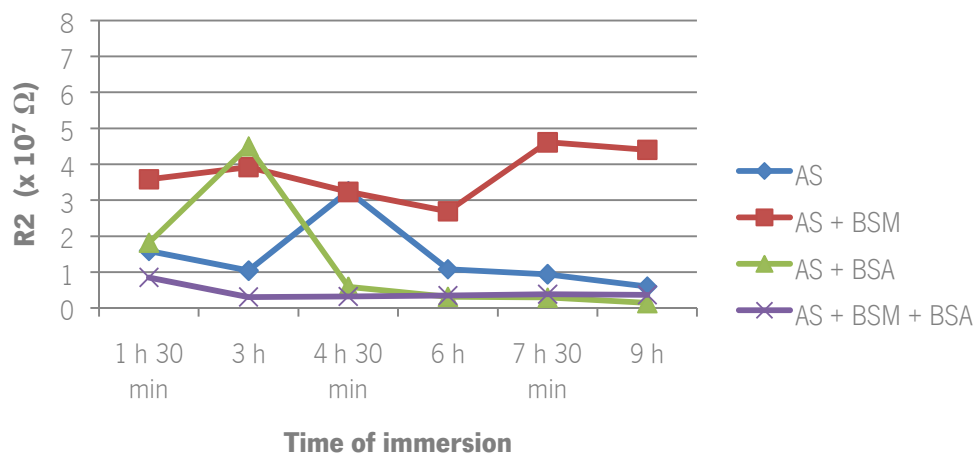


Figure 13 - Barrier film resistance (R2) registered for the EIS experiments performed with anodized samples, at different immersion times.

For the same solution, the values for R2 demonstrated by the anodized samples are in general smaller than the ones exhibited by the etched samples, except for the AS + BSM solution.

This indicates that this oxide film differs according to the surface treatment. On the anodized samples, this layer is covered with two others; therefore it is less exposed to the ambient air, making it possible that the characteristics of this layer to be different.

Between test solutions, the values obtained for the AS + BSM are the highest, in the case of the anodized samples, and the lowest for the other samples. It may reveal that the mucin adsorbs to the porous surface of the anodized samples and obstructs the passage of current.

Throughout the time of immersion the values for this parameter oscillate, making it not able to conclude anything about the behavior.

It is also important to refer that the highest values for the first graphic (namely the last value of the AS + BSM and the highest value of the AS curve), are also the ones that have the highest standard deviation, for that, they are not as relevant as the others, that seem to follow the general behavior of the respective curve.

On Figure 14, as the last value of the AS curve is much higher than the other values for the same curve, having a standard deviation of 71,4; it is safe to say that this value do not describe accurately the behavior of the sample under the test condition. For this reason, and to be able to reduce the graphic scale to one near the scale adopted in Figure 16 for comparison purposes, this value is withdrawn on Figure 15.

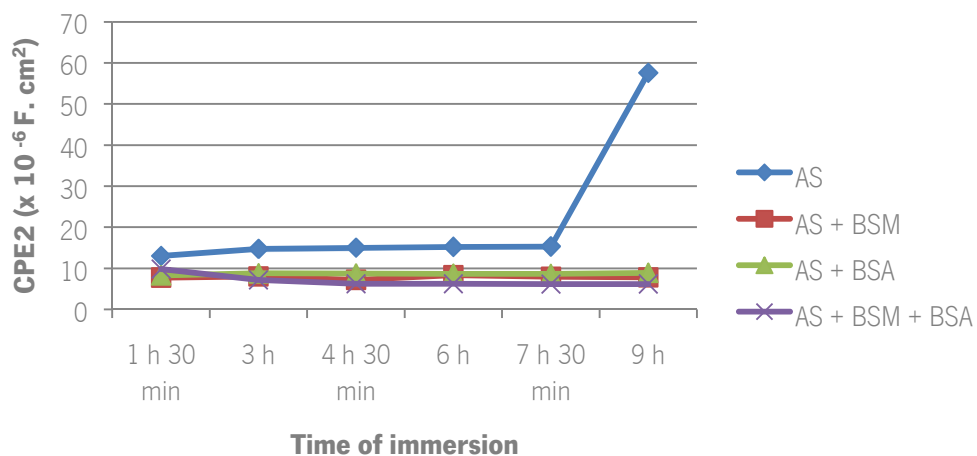


Figure 14 - Barrier film capacitance (CPE2) registered for the EIS experiments performed with etched samples, at different immersion times.

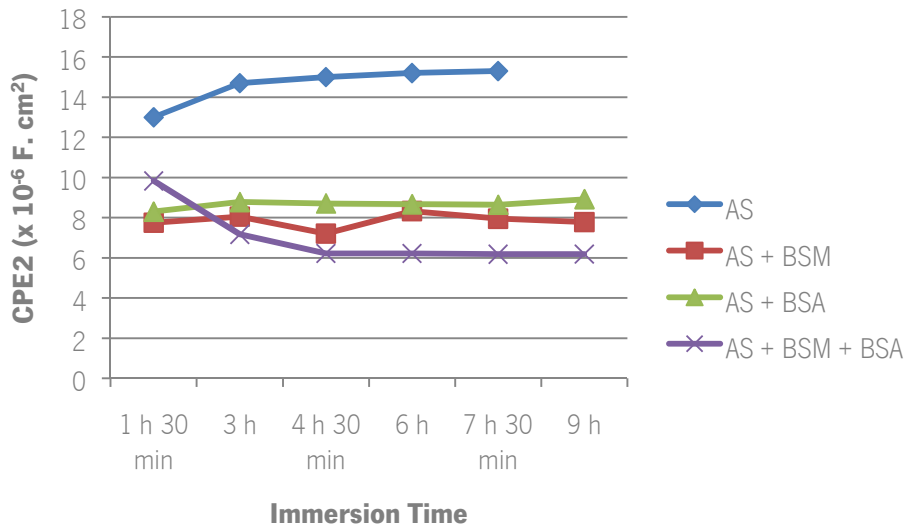


Figure 15 - Barrier film capacitance (CPE2) registered for the EIS experiments performed with etched samples, at different immersion times.

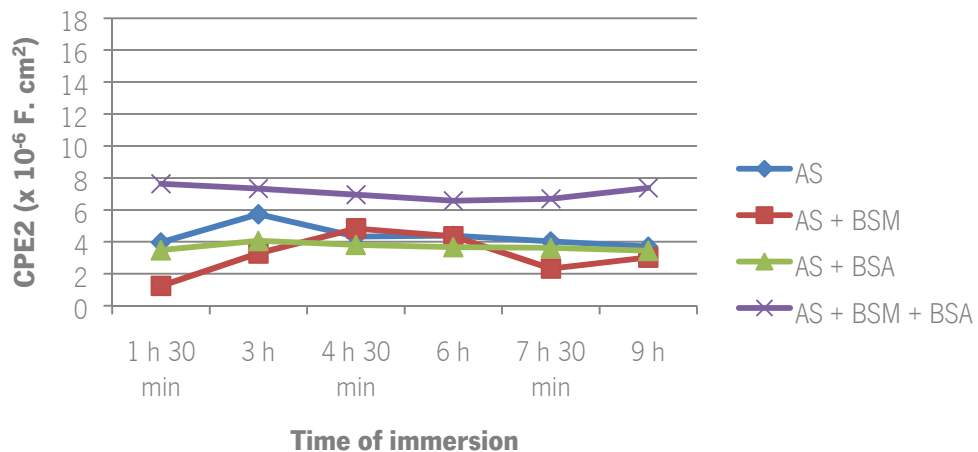


Figure 16 - Barrier film capacitance (CPE2) registered for the EIS experiments performed with anodized samples, at different immersion times.

Comparing between surfaces, the values for CPE2 demonstrated by the anodized samples are smaller than the ones exhibited by the etched samples, except in the case where it's used the mixed solution. Although the values indicate a higher capacitive behavior in the case of the anodized samples, which may also show higher protection for these samples, when considering the standard deviation the values for CPE2 for anodized and etched samples are close,. This indicates that the difference of the barrier film behavior for both samples is not significant when in the presence of both proteins.

In general, this barrier film is more efficient in the case of the etched samples, regarding the protection on the metal to corrosion.

Between test solutions, the values obtained for the AS + BSM are the smallest for the tests performed using the anodized samples while for the etched samples the smaller corresponds to the tests with the solution with the two proteins. At this point and regarding the proteins influence no conclusions should be taken since the solution is not in direct contact with this layer.

Throughout immersion time, the curves of this parameter are more or less stable.

4.2.5 Porous Layer

The porous layer is represented in every equivalent circuit by R1 and CPE1. Since it refers to a porous film formed on top of the natural oxide film of titanium, the values obtained for the fitting for each EIS test are comparable and presented on Figures 17, 18, 19 and 20.

The values for the standard deviation for R1 are between 0,001 and 0,28 for the etched samples and 0,3 to 38,8 for the anodized samples, being these higher values applicable to the higher values presented on Figure 18.

The values for the standard deviation for CPE1 are between 0,35 and 4,9 for the etched samples and 0,15 to 6,94 for the anodized samples, being these higher values applicable to the higher values presented on Figure 18.

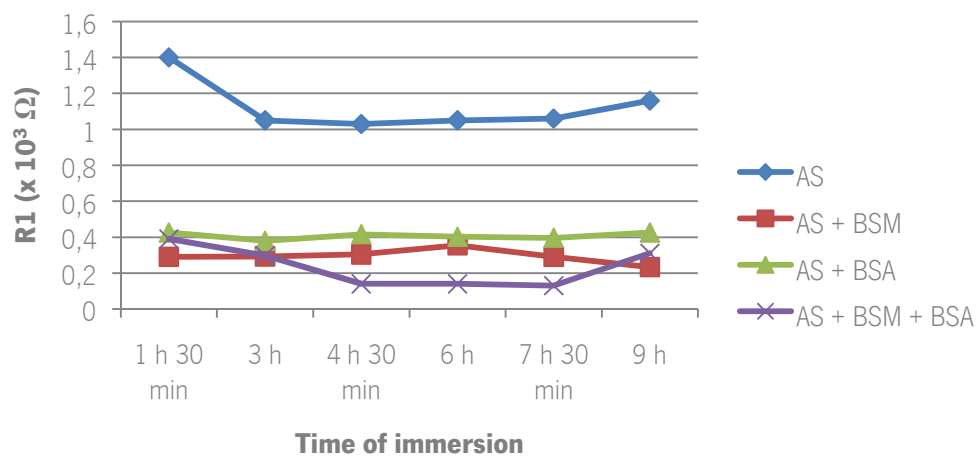


Figure 17 - Porous layer resistance (R1) registered for the EIS experiments performed with etched samples, at different immersion times.

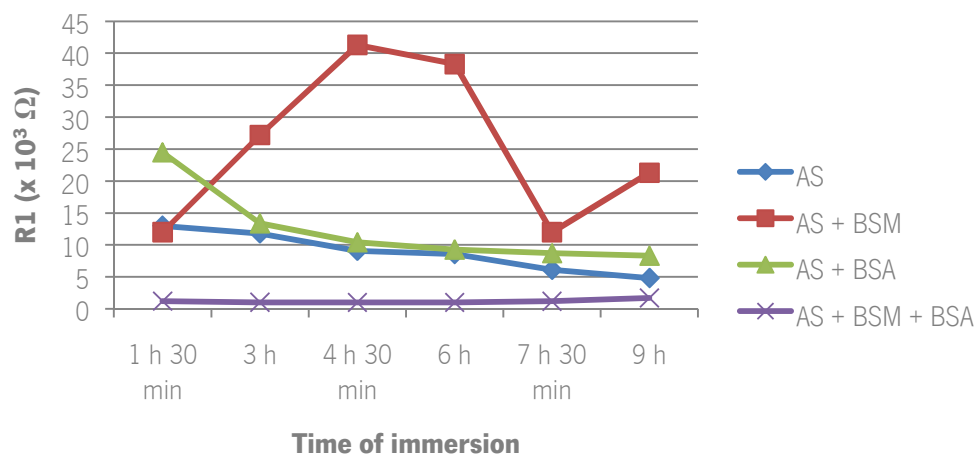


Figure 18 - Porous layer resistance (R1) registered for the EIS experiments performed with anodized samples, at different immersion times.

This is the last layer of the etched samples.

Comparing the values of R1 for the same solution, they are significantly higher for the anodized samples. It is understandable, for what is already known of this layer in these samples, given the fact that it is thicker than the last one and compacter than the following. Comparing with the etched samples, it is possible to conclude that this layer differs according to the surface treatment. Since for these samples, this layer is in direct contact with the immersion solution, it is not possible to compare between topographies, or its influence to protein adsorption.

Between test solutions, the values obtained for the mixed solution are the smallest, for both samples. It may reveal that, for this layer, single proteins have more influence than the mixture of both. It may indicate that the interaction between proteins does not favor the adsorption to the material.

For the etched samples the curves are more or less stable, so it is possible to observe that throughout the time of immersion there are no significant differences that may lead to any conclusions about the influence of the time of immersion in the resistive behavior in this case.

For the anodized samples, throughout the time of immersion the values for this parameter oscillate, making it not able to conclude about the behavior.

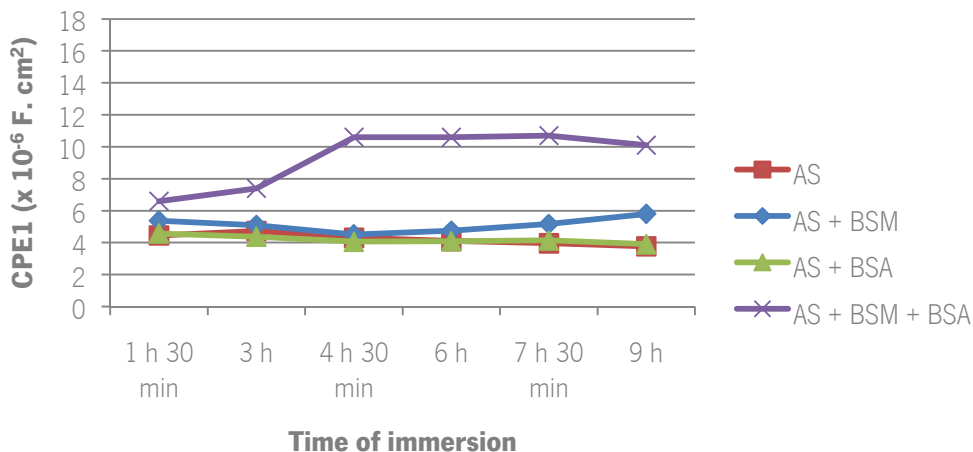


Figure 19 - Porous layer capacitance (CPE1) registered for the EIS experiments performed with etched samples, at different immersion times.

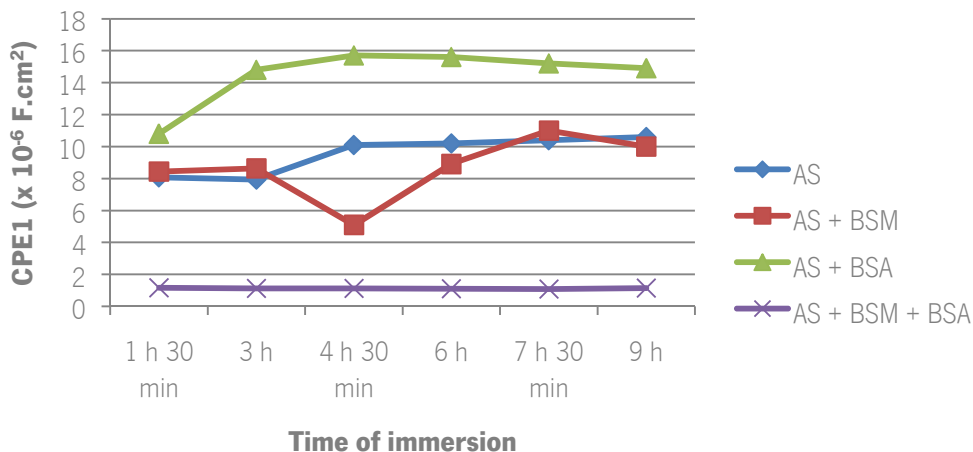


Figure 20 - Porous layer capacitance (CPE1) registered for the EIS experiments performed with anodized samples, at different immersion times.

For the same solution, the values for CPE1 demonstrated by the anodized samples are higher than the ones exhibited by the etched samples, except in the case where it's used the mixed solution.

The overall perspective leads to the conclusion that this layer is much stronger in the case of the anodized samples. As for the case using both proteins, since it is the last level of the etched surface, the direct contact with the proteins may lead to higher adsorption of those to this type of surface.

Between test solutions, the values obtained for the AS + BSM + BSA are the smallest for the tests performed using the anodized samples while for the etched samples the smaller corresponds to the tests performed with the solution containing albumin. Only when comparing to the last layer of the anodized samples it is possible to conclude about the proteins tendency to adsorb more to one surface or another.

Throughout immersion time the behavior of this parameter (CPE1) does not lead to any conclusion.

Comparing the values of CPE1 with CPE2, the first has higher values, which indicates the higher capacitive effect, it is possible to infer that the porous layer is more effective than the barrier film, for the anodized samples. The opposite occurs for the etched samples.

The comparison between the resistances indicates a different idea. The values of R2 are higher than R1 for the etched samples and the reverse occurs for the anodized ones. Since it refers

to the solution embed in the layer, the resistive behavior is higher in the porous layer for the anodized samples and the barrier film is more protective of the etched surface.

4.2.6 Outer Porous Layer

The outer porous layer is present only for anodized samples, represented by R3 and CPE3 in the equivalent circuit. It refers to a porous film formed on the most external part of the material. The values obtained for the fitting for each EIS test are presented on Figures 21 and 22. The values of the standard deviation for the R3 are between 0,011 and 31; for CPE3 are between 0,157 and 9,38.

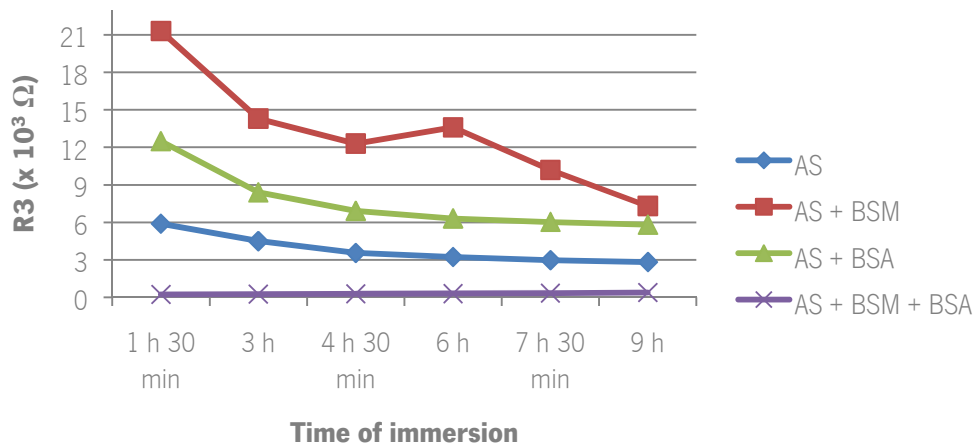


Figure 21 - Outer porous layer resistance (R3) registered for the EIS experiments performed with the anodized samples, at different immersion times.

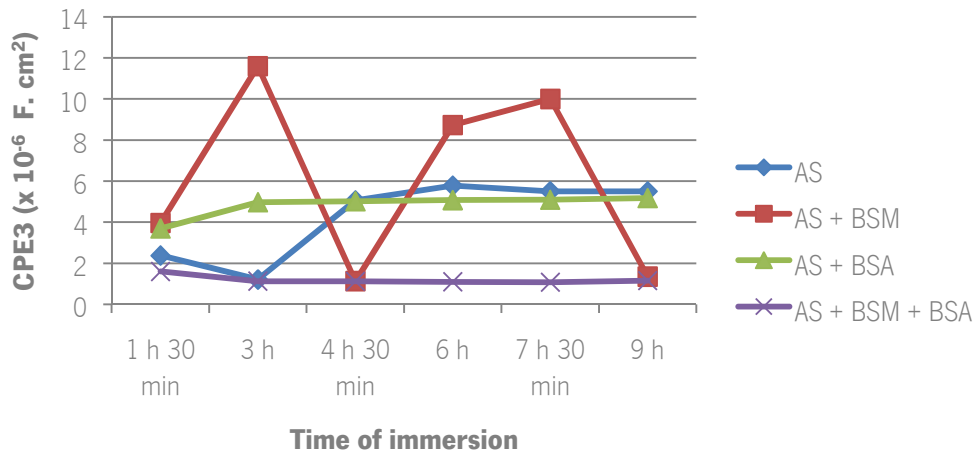


Figure 22 - Outer porous layer capacitance (CPE3) registered for the EIS experiments performed with anodized samples, at different immersion times.

These Figures aim to present the values obtained by the fitting in a manner to facilitate the assessment of the influence of the presence of the used proteins, isolated and mixed.

Relative to the resistive behavior of this layer, the values of R3 decrease throughout the immersion time except for the tests with the mixed solution. Although the values of this curve increase along with the time of immersion for this condition, they are also the smallest. The highest values for R3 refer to the experiments with mucin. Maybe the protein adsorbs to the inside part of the pores, making it harder for the current to pass. This theoretical explanation is supported by the CPE3 values, which are higher to the experiments with mucin, despite the irregular curve. The lowest values of CPE3 are also related to the experiments using both proteins. It may support the idea that the interaction between proteins is not favorable to the adsorption.

Comparing the three layers (barrier film, porous layer and outer porous layer) for the anodized samples, the CPE3 are smaller than CPE1 (except for the mixed solution, in which case is similar) but higher than CPE2, for all immersion solution. This indicates that this layer is stronger than the barrier film but weaker than the porous layer. The fact that this last layer is thicker than the native film and that the porous layer was referred as being compact, in the case of the anodized samples, could be an explanation to this behavior.

In the case of the samples in analysis, the values of the resistances are higher for R1 (except for the case of the mixed solution), followed by R3 and at last R2. This was already expected once the last layer has bigger pores, so the solution can spread through them and simplify the passage of current. The next layer, represented by R1 and CPE1 is compact therefore offering

the highest resistance to the current. The native oxide film is represented by R2 and CPE2 and since it is thinner, its resistive behavior is the weaker.

Apparently, when comparing the affinity of the proteins with the layer that has more contact with the solution, for the different test surfaces, it is possible to conclude that there is no significant difference, except for the ultimate condition. When using both proteins it seems that etched samples reveal more affinity to the deposition of the proteins onto the surface.

4.2.7 Irregular Mucin Layer

This layer is present only when using the AS + BSM solution and with anodized samples, represented by R4 and CPE4 in the equivalent circuit from Figure 9. It refers to a protein deposit formed on the most external part of the material. The values obtained for the fitting for each EIS test are presented on Figure 23. The values for the standard deviation are between 3,46 and 14,5 for R4 and 0,15 and 9,19 for CPE4.

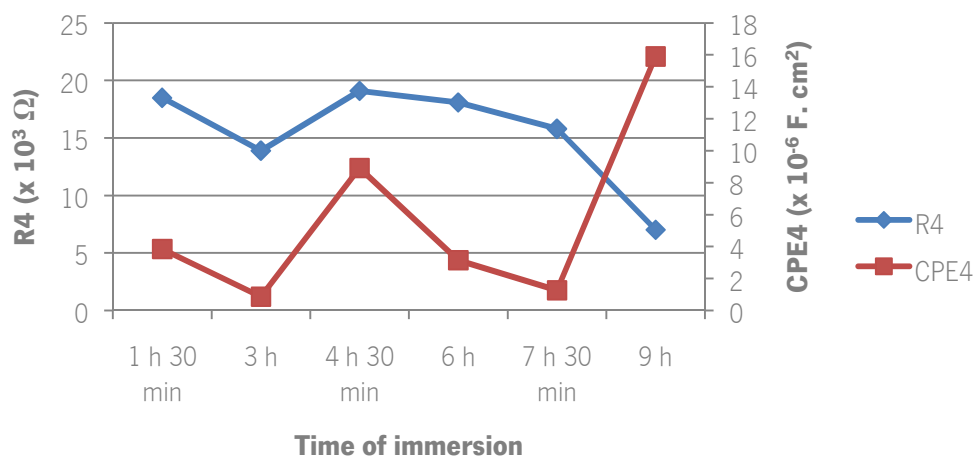


Figure 23 - Irregular mucin layer resistance (R4) and capacitance (CPE4) registered for the EIS experiments performed immersing anodized samples in an AS + BSM solution, at different immersion times.

The fitting performed on the data collected from the experiments performed in this conditions revealed this extra layer.

The existence of this layer may lead to the conclusion that this surface treatment has more affinity for this protein to adsorb, since it appears to form a coating on the surface. Through the fitting it is possible to consider that the layer is composed by two circuit elements: one resistance

(R4) that simulates the resistive behavior of the solution embed in the protein, and a constant phase element (CPE4), that reflects the capacitive effect of the protein layer. At first sight, this conclusion is validate by the increasing values of CPE4 throughout the immersion time, which indicates that the longer the study material is immersed in the test solution, the higher the capacitive ability. It leads to the thought that perhaps the protein deposition also increases with time.

In general the values of R4 are higher than the other resistances values, except for the case of R1 when using mucin, which indicates that this layer has a stronger resistive behavior than the other ones. In the case of the porous film, since it is compact it is natural to have a more resistive behavior. The CPE4 has similar behavior to CPE3.

Since this layer does not occur for the etched samples, it is presumed that the anodized treatment is more appealing to the mucin adsorption.

Chapter 5 | Conclusions and Future Work

Regarding the main objectives of this work, it is not possible to state definite conclusions about the surface treatments and its influence on the proteins ability to adsorb. Therefore, only assumptions can be taken.

Proteins seem to have more affinity with the anodized surfaces. Mucin, in particular, demonstrated high capacity to adsorb to this surface, proving its ability to form a diffuse film, as stated on the literature. The presence of the porous layer on the anodized treated samples made it more appropriate for protein deposition. It could facilitate the migration of osteoblasts, as so osteointegration. For the etched treatment, the proteins often presented similar behavior, not adhering to the surface.

As mucin alone formed a film on the anodized surface and when blended with albumin the film is not present, it is possible to conclude that albumin influences the ability of mucin adsorb to these surfaces. According to the literature, albumin would strongly affect properties of adsorbed layers of BSM. It is possible to suspect that the proteins bond under these test conditions (absence of light, 37° C, 9 hours of immersion time), forming small agglomerates and possibly precipitate; therefore they do not adhere to the surface of the working electrode. As the interaction between these two proteins is not fully understood more work is needed to confirm this idea. In fact, both proteins are present on the locus of the implant. If there weren't any other factors to account (such as inflammation, pH, age of the patient, and so on), it would be expected that, when using any of these treatments on an actual dental implant, at least on the first 9 hours, no protein layer would be formed.

Regarding the proteins influence on the corrosion behavior of titanium specimens immersed in solutions prepared with Fusayama artificial saliva, only few conclusions are possible to state. When testing with the solution containing only BSM, the formation of one extra layer on the anodized samples could indicate that it protects the surface from the influence of ions that may occur in the surrounding area. On the other hand, in these conditions, BSA does not have any distinct behavior alone and interferes with the mucin layer formation. To confirm this assumption different condition tests should be assumed, as such increasing the immersion time to observe if the protein inhibits the formation of the biologic film or just delays it.

As the natural concentration of albumin in the human blood is ten times higher than the one used in this work, perhaps it would be interesting to investigate the influence of increasing concentration of albumin, up to its natural concentration, using the same conditions as in this work.

Also, some experiments with fibrin (protein that initiates the osteointegration) could reveal more about this possible ability of this surface.

To assess more about the influence of the test solution in the corrosion of titanium potentiodynamic test could bring interesting information, regarding corrosion rate for instance.

References

1. **Surgeons, American Association of Oral and Maxillofacial.** Conditions & Treatments. *American Association of Oral and Maxillofacial Surgeons*. [Online] American Association of Oral and Maxillofacial Surgeons, 2005-2008. [Cited: Agosto 9, 2011.] http://www.aaoms.org/dental_implants.php.
2. Dental Implants. *Strem Resnick Tetelman & Young - wole life dentistry*. [Online] PBHS, 2010. [Cited: Agosto 10, 2011.] <http://www.wholelifedentistry.com/dental-services-lyndhurst-oh/implant-surgery.html>.
3. **Le Guéhennec, L., et al.** Surface treatments of titanium dental implants for rapid osseointegration. *Dental Materials*. 2007, Vol. 23, pp. 844-854.
4. **Yu, Wei-qiang, Qiu, Jing and Zhang, Fu-qiang.** In vitro corrosion study of different TiO₂ nanotube layers on titanium in solution with serum proteins. *Colloids and Surfaces B: Biointerfaces*. 2011, Vol. 84, pp. 400-405.
5. **Wehmeyer, Jennifer, et al.** Dynamic adsorption of albumin on nanostructured TiO₂ thin films. *Materials Science and Engineering C*. 2010, Vol. 30, pp. 277-282.
6. **Anusavice, Kenneth J.** *Phillips' Science of Dental Materials*. Missouri : Elsevier, 2003.
7. **Hobkirk, John A., Watson, Roger M. and Searson, Lloyd J. J.** *Introducing Dental Implants*. s.l. : Churchill Livingstone, 2003.
8. **Pye, A. D., et al.** A review of dental implants and infection. *Journal of Hospital Infection*. 2009, Vol. 72, pp. 104-110.
9. **Ratner, Buddy D., et al.** *Biomaterials Science: An Introduction to Materials in Medicine*. London : Academic Press, 1996.
10. Las Vegas Dental Implants. *Las Vegas Dental Implants*. [Online] 2010. <http://lasvegasdentalimplants.org/wp-content/uploads/2010/08/dental-implant-anatomy2-300x241.jpg>.
11. **Elias, C. N., Figueira, D. C. and Rios, P. R.** Influence of the coating material on the loosening of dental implant abutment screw joints. *Materials Science and Engineering C*. 2006, Vol. 26.
12. [Online] [Cited: Agosto 10, 2011.] <http://lasvegasdentalimplants.org/wp-content/uploads/2010/08/dental-implant-anatomy2-300x241.jpg>.
13. **Baqain, Zaid H., Moqbel, Wael Y. and Sawair, Faleh A.** Early dental implant failure: risk Factors. *British Journal of Oral and Maxillofacial Surgery*. 2011.
14. **Rosales-Leal, J.I., et al.** Effect of roughness, wettability and morphology of engineered titanium surfaces on osteoblast-like cell adhesion. *Colloids and Surfaces A: Physicochemical and Engineering Aspects*. 2010, Vol. 365, pp. 222-229.
15. **González, J. E. G. and Mirza-Rosca, J. C.** Study of the corrosion behaviour of titanium and some of its alloys for biomedical and dental implant applications. *Journal of Electroanalytical Chemistry*. 1999, Vol. 471, pp. 109-115.

16. **Krupa, D., et al.** Effect of calcium-ion implantation on the corrosion resistance and biocompatibility of titanium. *Biomaterials*. 2001, Vol. 22, pp. 2139-2151.
17. **Song, Ho-Jun, et al.** The effects of spark anodizing treatment of pure titanium metals and titanium alloys on corrosion characteristics. *Surface & Coatings Technology*. 2007, Vol. 201, pp. 8738-8745.
18. **Kumar, Satendra and Narayanan, T. S. N. Sankara.** Corrosion behaviour of Ti-15Mo alloy for dental implant applications. *Journal of Dentistry*. 2008, Vol. 36, pp. 500-507.
19. **Zhu, Xiaolong, Kim, Kyo-Han and Jeong, Yongsoo.** Anodic oxide films containing Ca and P of titanium biomaterial. *Biomaterials*. 2001, Vol. 22, pp. 2199-2206.
20. **Chen, Z. X., et al.** Microstructure and shear fracture characteristics of porous anodic TiO₂ layer before and after hot water treatment. *Applied Surface Science*. 2011, Vol. 257, pp. 7254-7262.
21. **Demetrescu, I., Pirvu, C. and Mitran, V.** Effect of nano-topographical features of Ti/TiO₂ electrode surface on cell response and electrochemical stability in artificial saliva. *Bioelectrochemistry*. 2010, Vol. 79, pp. 122-129.
22. **Kuromoto, Neide K., Simão, Renata A. and Soares, Gloria A.** Titanium oxide films produced on commercially pure titanium by anodic oxidation with different voltages. *Materials Characterization*. 2007, Vol. 58, pp. 114-121.
23. **Song, Ho-Jun, et al.** Surface characteristics and bioactivity of oxide films formed by anodic spark oxidation on titanium in different electrolytes. *Journal of material processing technology*. 2009, Vol. 209, pp. 864-870.
24. **Kopac, Turkan and Bozgeyyik, Kadriye.** Effect of surface area enhancement on the adsorption of bovine serum albumin onto titanium dioxide. *Colloids and Surface B: Biointerfaces*. 2010, Vol. 76, pp. 265-271.
25. **Trethewey, K. R. and Chamberlain, J.** *Corrosion from Science and Engineering*. United Kingdom : Longman, 1995.
26. **Aparicio, Conrado, Padrós, Alejandro and Gil, Francisco-Javier.** In vivo evaluation of micro-rough and bioactive titanium dental implants using histometry and pull-out tests. *Journal of the mechanical behavior of biomedical materials*. 2011.
27. **Cui, X., et al.** Preparation of bioactive titania films on titanium metal via anodic oxidation. *Dental Materials*. 2009, Vol. 25, pp. 80-86.
28. **Schweitzer, Philip A.** *Fundamentals of Corrosion*. s.l. : CRC Press, 2010.
29. **MacDonald, D. D. and Kubre, M. C. H.** Electrochemical Impedance Techniques in Corrosion Science. *Electrochemical Corrosion testing*. s.l. : Florioan Mansfeld ang Ugo Betrocci, Eds., 1981, pp. 110-149.
30. **Marino, Cláudia E. B. and Mascaro, Lucia Helena.** EIS characterization of a Ti-dental implant in artificial saliva media: dissolution process of the oxide barrier. *Journal of Electroanalytical Chemistry*. 2004, Vol. 568, pp. 115-120.
31. **Vieira, A. C., et al.** Influence of pH and corrosion inhibitors on the tribocorrosion of titanium in artificial saliva. *Wear*. 2006, Vol. 261, pp. 994-1001.

32. **Venture, XProduction.** General Dentistry- Implants. *My Dental Health*. [Online] XProduction Venture, 2008. [Cited: Agosto 10, 2011.] http://www.mydentalhealth.net/dental_implants.html.
33. **Schipper, Raymond G., Silletti, Erika and Vingerhoeds, Monique H.** Saliva as a researchd material: Biochemical, physicochemical and practical aspects. *Archives of Oral Biology*. 2007, Vol. 52, pp. 1114-1135.
34. **Carvalho, Ricardo and Brett, Christopher M. A.** Influência da Mucina no mecanismo de corrosão de uma amálgama dentária em saliva artificial. *Corrosão e Protecção de Matriais*. 2008, Vol. 27, pp. 108-113.
35. **Virtanen, S., et al.** Special modes of corrosion under physiological and simulated physiological conditions. *Acta Biomaterialia*. 2008, Vol. 4, pp. 468-476.
36. **Petersson, Ingela U., et al.** Semi conducting properties of titanium dioxide surface on titanium implants. *Biomaterials*. 2009, Vol. 30, pp. 4471-4479.
37. **Cheng, Xiaoliang and Roscoe, Sharon.** Corrosion behavior of titanium in the presence of calcium phosphate and serum proteins. *Biomaterials*. 2005, Vol. 26, pp. 7350-7356.
38. **Cvijovic-Alagic, I., et al.** Wear and corrosion behaviour of Ti-13Nb-13Zr and Ti-6Al-4V alloys in simulated physiological solution. *Corrosion Science*. 2011, Vol. 53, pp. 796-808.
39. **Vidal, C. Valero, Juan, A. Olmo and Muñoz, A. Igual.** Adsorption of bovine serum albumin on CoCrMo surface: Effect of temperature and protein concentration. *Colloids and Surfaces B: Biointerfaces*. 2010, Vol. 80, pp. 1-11.
40. **Takemoto, Shinji, et al.** Corrosion behavior and surface characterization of titanium in solution containing fluoride and albumin. *Biomaterials*. 2005, Vol. 26, pp. 829-837.
41. **Svensson, Olof and Arnebrant, Thomas.** Mucin layers and multilayers - Physicochemical properties and applications. *Current Opinion in Colloidal & Interface Science*. 2010, Vol. 15, pp. 395-405.
42. **Lundin, Maria, et al.** Comparison of the adsorption kinetics and surface arrangement of "as received" and purified bovine submaxillary gland mucin (BSM) on hydrophilic surfaces. *Journal of Colloid and Interface Science*. 2009, Vol. 336, pp. 30-39.
43. **Bansil, Rama and Turner, Bradley S.** Mucin structure, aggregation, physiological functions and biomedical applications. *Current Opinion in Colloid and Interface Science*. 2006, Vol. 11, pp. 164-170.
44. **Huang, Her-Hsiung.** Effect of fluoride and albumin concentration on the corrosion behavior of Ti-6Al-4V alloy. *Biomaterials*. 2003, Vol. 24, pp. 275-282.
45. **Jansson, Eva and Tengvall, Pentti.** Adsorption of albumin and IgG to porous and smooth titanium. *Colloids and Surfaces B: Biointerfaces*. 2004, Vol. 35, pp. 45-51.
46. **Barrias, Cristina C., et al.** The correlation between the adsorption of adhesive proteins and cell behaviour on hydroxyl-methyl mixed self-assembled monolayers. *Biomaterials*. 2009, Vol. 30, pp. 307-316.
47. **Liao, Wei, et al.** FTIR-ATR detection of proteins and small molecules through DNA conjugation. *Sensors and Actuators*. 2006, Vol. 114, pp. 445-450.

48. **Wood, B. R., et al.** Fourier transform infrared (FTIR) spectral mapping of the cervical transformation zone, and dysplastic squamous epithelium. *Gynecologic Oncology*. 2004, Vol. 93, pp. 59-68.
49. **Liu, C. L., et al.** In vitro corrosion degradation behaviour of Mg-Ca alloy in the presence of albumin. *Corrosion Science*. 2010, Vol. 52, pp. 3341-3347.
50. **Mueller, H. J. and Hirthe, R. W.** Electrochemical characterization and immersion corrosion of a consolidated silver dental biomaterial. *Biomaterials*. 2001, Vol. 22, pp. 2635-2646.
51. **Oliva, Fabiana Y., Cámara, Osvaldo R. and Avalué, Lucía B.** Adsorption of human serum albumin on electrochemical titanium dioxide electrodes: Proteins-oxide surface interaction effects studied by electrochemical techniques. *Journal of Electroanalytical Chemistry*. 2009, Vol. 633, pp. 19-34.
52. **Orazem, M. E. and Tribollet, B.** *Electrochemical Impedance Spectroscopy*. s.l. : Wiley, 2008.
53. **Oliveira, N.T.C., et al.** Photo-electrochemical and impedance investigation of passive layers grown anodically on titanium alloys. *Electrochimica Acta*. 2004, pp. 4563-4576.
54. **Vasilescu, C., et al.** Characterisation and corrosion resistance of the electrodeposited hydroxyapatite and bovine serum albumin/hydroxyapatite films on Ti-6Al-4V-1Zr alloy surface. *Corrosion Science*. 2011, pp. 992-999.
55. **Ibris, Neluta and Rosca, Julia Claudia Mirza.** EIS study of Ti and its alloys in biological media. *Journal of Electroanalytical chemistry*. 2002, pp. 53-62.
56. **Huang, Yuelong, et al.** Evaluation of the corrosion resistance of anodized aluminium 6061 using electrochemical impedance spectroscopy (EIS). *Corrosion science*. 2008, pp. 3569-3575.
57. **Hiramoto, S. and Mischler, S.** The influence of proteins on the fretting-corrosion behaviour of a Ti6Al4V alloy. *Wear*. 2006, Vol. 261, pp. 1002-1011.
58. **Figueira, N., et al.** Corrosion behaviour of NiTi alloy. *Electrochimica Acta*. 2009, Vol. 54, pp. 921-926.
59. **Tosatti, S., et al.** Peptide functionalized l-lysine-g-poly(ethylene glycol) on titanium: resistance to protein adsorption in full heparinized human blood plasma. *Biomaterials*. 2003, Vol. 24, pp. 4949-4958.
60. **Huang, Her-Hsiung and Lee, Tzu-Hsin.** Electrochemical impedance spectroscopy study of Ti-6Al-4V alloy in artificial saliva with fluoride and/or bovine albumin. *Dental Materials*. 2005, Vol. 21, pp. 749-755.

Appendix

Appendix 1 – Tables with the values used for the graphics presented on chapter 4 and respective standard deviation.

Appendix 1

Tables with the values used for the graphics presented on chapter 4 and respective standard deviation.

In this appendix are presented the tables with the values used for the constructions of the graphics presented on chapter 4 (*Results*) with the respective standard deviations.

Table 7 - Electrolyte resistance (R_{sol}) registered for the EIS experiments, at different immersion times.

Time of immersion	$R_{sol} (x10^2 \Omega)$							
	Etched samples				Anodized samples			
	AS	AS + BSM	AS + BSA	AS + BSM + BSA	AS	AS + BSM	AS + BSA	AS + BSM + BA
1 h 30 min	1.59 ± 0.0092	1.51 ± 0.08	1.59 ± 0.0019	1.48 ± 0.077	1.74 ± 0.039	1.75 ± 0.073	1.62 ± 0.01	1.51 ± 0.05
3 h	1.56 ± 0.0097	1.46 ± 0.07	1.55 ± 0.0097	1.44 ± 0.0088	1.67 ± 0.019	1.59 ± 0.036	1.57 ± 0.0097	1.48 ± 0.0595
4 h 30 min	1.54 ± 0.01	1.44 ± 0.07	1.53 ± 0.03	1.38 ± 0.088	1.64 ± 0.013	1.53 ± 0.045	1.54 ± 0.0095	1.46 ± 0.0656
6 h	1.525 ± 0.0024	1.42 ± 0.07	1.51 ± 0.03	1.35 ± 0.092	1.61 ± 0.026	1.49 ± 0.05	1.52 ± 0.0072	1.44 ± 0.063
7 h 30 min	1.52 ± 0.012	1.398 ± 0.069	1.49 ± 0.03	1.32 ± 0.09	1.599 ± 0.028	1.465 ± 0.056	1.5 ± 0.0072	1.42 ± 0.06
9 h	1.504 ± 0.014	1.42 ± 0.024	1.49 ± 0.03	1.25 ± 0.06	1.58 ± 0.029	1.45 ± 0.048	1.49 ± 0.0061	1.4 ± 0.0525

Table 8 - Barrier film resistance (R_2) registered for the EIS experiments, at different immersion times.

Time of immersion	$R_2 (x10^7 \Omega)$							
	Etched samples				Anodized samples			
	AS	AS + BSM	AS + BSA	AS + BSM + BSA	AS	AS + BSM	AS + BSA	AS + BSM + BSA
1 h 30 min	3.13 ± 1.42	1.89 ± 1.52	3.23 ± 2.06	1.76 ± 0.96	1.59 ± 1.69	3.58 ± 0.827	1.82 ± 1.27	0.85 ± 0.025
3 h	2.77	1.52	3.87	2.44	1.04	3.92	4.50	0.307

	±0.37	±1.02	±2.72	±1.7	±1.04	±1.57	±6.51	±0.0153
4 h 30 min	3.6 ±0.99	1.29 ±0.885	2.82 ±0.616	3.1 ±2.4	3.25 ±4.63	3.23 ±1.53	0.593 ±0.537	0.322 ±0.00971
6 h	5.3 ±1.15	1.23 ±0.992	2.86 ±0.46	3.3 ±2.3	1.08 ±1.10	2.69 ±3.57	0.315 ±0.137	0.347 ±0.0231
7 h 30 min	6.9 ±3.2	1.13 ±1.02	3.09 ±0.641	3.2 ±1.8	0.94 ±0.734	4.61 ±3.57	0.292 ±0.125	0.385 ±0.0568
9 h	3.82 ±1.2	4.80 ±3.39	3.85 ±1.84	2.6 ±0.59	0.6 ±0.433	4.40 ±2.01	0.14 ±0.135	0.369 ±0.0253

Table 9 - Barrier film capacitance (CPE2) registered for the EIS experiments, at different immersion times.

Time of immersion	CPE2 (x10 ⁶ F. cm ²)							
	Etched samples				Anodized samples			
	AS	AS + BSM	AS + BSA	AS + BSM + BSA	AS	AS + BSM	AS + BSA	AS + BSM + BSA
1 h 30 min	13 ±2.12	7.75 ±1.89	8.3 ±1.32	9.83 ±0.919	3.97 ±2.82	1.24 ±0.247	3.48 ±1.78	7.63 ±1.6
3 h	14.7 ±1.53	8.05 ±1.65	8.78 ±0.197	7.17 ±3.74	5.73 ±1.9	3.28 ±2.77	4.06 ±2.52	7.34 ±1.89
4 h 30 min	15 ±1	7.21 ±0.997	8.71 ±0.67	6.22 ±5.31	4.33 ±3.38	4.84 ±3.64	3.81 ±2.35	6.95 ±1.91
6 h	15.2 ±1.26	8.33 ±2.03	8.67 ±0.659	6.22 ±5.3	4.38 ±3.53	4.35 ±3.68	3.67 ±2.26	6.57 ±2.63
7 h 30 min	15.3 ±1.42	7.95 ±1.48	8.64 ±0.736	6.18 ±5.25	4.03 ±3.37	2.32 ±1.89	3.62 ±2.21	6.7 ±3
9 h	57.6 ±71.4	7.78 ±0.6	8.92 ±1.25	6.19 ±5.24	3.7 ±3.03	3.02 ±0.804	3.44 ±2.05	7.37 ±4.08

Table 10 – Porous layer resistance (R1) registered for the EIS experiments, at different immersion times.

Time of immersion	R1 ($\times 10^3 \Omega$)							
	Etched samples				Anodized samples			
	AS	AS + BSM	AS + BSA	AS + BSM + BSA	AS	AS + BSM	AS + BSA	AS + BSM + BSA
1 h 30 min	1.4 ± 0.181	0.29 ± 0.0279	0.425 ± 0.0405	0.39 ± 0.28	13 ± 10	12 ± 20	24.5 ± 14	1.21 ± 0.335
3 h	1.05 ± 0.248	0.293 ± 0.0128	0.379 ± 0.0741	0.297 ± 0.21	11.8 ± 9.8	27.2 ± 20.7	13.4 ± 5.46	1.03 ± 0.301
4 h 30 min	1.03 ± 0.311	0.304 ± 0.0604	0.416 ± 0.0139	0.14 ± 0.12	9.07 ± 8.95	41.3 ± 38.7	10.4 ± 3.27	0.995 ± 0.309
6 h	1.05 ± 0.234	0.354 ± 0.144	0.402 ± 0.0108	0.14 ± 0.113	8.57 ± 8.79	38.3 ± 38.8	9.26 ± 2.29	1 ± 0.418
7 h 30 min	1.06 ± 0.299	0.291 ± 0.0711	0.396 ± 0.0149	0.13 ± 0.1	6.1 ± 5.26	12 ± 12.7	8.70 ± 1.72	1.19 ± 0.683
9 h	1.16 ± 0.222	0.233 ± 0.0573	0.425 ± 0.0794	0.31 ± 0.1	4.81 ± 3.52	21.3 ± 15	8.31 ± 1.28	1.72 ± 1.49

Table 11 – Porous layer capacitance (CPE1) registered for the EIS experiments, at different immersion times.

Time of immersion	CPE1 ($\times 10^6 \text{ F. cm}^2$)							
	Etched samples				Anodized samples			
	AS	AS + BSM	AS + BSA	AS + BSM + BSA	AS	AS + BSM	AS + BSA	AS + BSM + BSA
1 h 30 min	4.45 ± 1.39	5.37 ± 1.1	4.58 ± 1.43	6.6 ± 4.9	8.08 ± 2.55	8.44 ± 2.3	10.8 ± 4.78	1.16 ± 0.173
3 h	4.73 ± 0.45	5.1 ± 1.02	4.37 ± 0.586	7.4 ± 4.7	7.94 ± 1.39	8.64 ± 1.69	14.8 ± 5.57	1.13 ± 0.157
4 h 30 min	4.3 ± 0.557	4.52 ± 1.06	4.06 ± 0.575	10.6 ± 2.5	10.1 ± 3.01	5.1 ± 6.01	15.7 ± 6.77	1.12 ± 0.166
6 h	4.1 ± 0.4	4.75 ± 0.631	4.09 ± 0.453	10.6 ± 2.4	10.2 ± 3.5	8.91 ± 5.68	15.6 ± 6.94	1.1 ± 0.187
7 h 30 min	3.96 ± 0.35	5.17 ± 0.514	4.14 ± 0.48	10.7 ± 2.3	10.4 ± 3.4	11 ± 2.89	15.2 ± 6.71	1.08 ± 0.196
9 h	3.77 ± 0.383	5.8 ± 1.22	3.9 ± 0.812	10.1 ± 2.34	10.6 ± 3.54	10 ± 2.89	14.9 ± 6.53	1.15 ± 0.15

Table 12 – Outer porous layer resistance (R1) and capacitance (CPE3) registered for the EIS experiments performed with anodized samples, at different immersion times.

Time of immersion	Anodized samples							
	AS	AS + BSM	AS + BSA	AS + BSM + BSA	AS	AS + BSM	AS + BSA	AS + BSM + BSA
	R3 ($10^3 \Omega$)				CPE3 (10^6 F. cm^2)			
1 h 30 min	5.89 ± 2.4	21.3 ± 31	12.5 ± 2.84	0.24 ± 0.035	2.38 ± 2.1	3.96 ± 5.1	3.7 ± 4.47	1.6 ± 0.173
3 h	4.50 ± 1.92	14.3 ± 17	8.40 ± 0.0967	0.253 ± 0.0738	1.21 ± 0.179	11.6 ± 9.38	4.98 ± 6.38	1.13 ± 0.157
4 h 30 min	3.56 ± 2.05	12.3 ± 16.2	6.92 ± 0.594	0.278 ± 0.011	5.06 ± 6.7	1.13 ± 0.643	5.02 ± 6.65	1.12 ± 0.166
6 h	3.23 ± 1.88	13.6 ± 19.5	6.31 ± 0.36	0.30 ± 0.0147	5.78 ± 7.9	8.73 ± 12.4	5.08 ± 6.86	1.1 ± 0.187
7 h 30 min	2.98 ± 1.64	10.2 ± 11.9	6.03 ± 0.238	0.341 ± 0.0188	5.5 ± 8.25	10 ± 14.7	5.1 ± 6.93	1.08 ± 0.196
9 h	2.83 ± 1.51	7.31 ± 9.86	5.81 ± 0.267	0.392 ± 0.0256	5.5 ± 7.36	1.35 ± 0.43	5.18 ± 7.12	1.15 ± 0.15

Table 13 – Irregular mucin layer resistance (R4) and capacitance (CPE4) registered for the EIS experiments performed immersing anodized samples in an AS + BSM solution, at different immersion times.

Time of immersion	Anodized sample (AS + BSM)	
	R4 ($10^3 \Omega$)	CPE4 (10^6 F. cm^2)
1 h 30 min	18.5 ± 9.48	3.85 ± 5.34
3 h	13.9 ± 13.36	0.86 ± 0.15
4 h 30 min	19.1 ± 14.5	8.92 ± 9.19
6 h	18.1 ± 14.3	3.15 ± 3.26
7 h 30 min	15.8 ± 13	1.26 ± 0.314
9 h	7.01 ± 3.46	15.9 ± 2.52